Front. Optoelectron. 2016, 9(2): 160–185
DOI 10.1007/s12200-016-0633-0

REVIEW ARTICLE

Recent advances in microwave photonics

Ming LI (✉), Ninghua ZHU (✉)

State Key Laboratory on Integrated Optoelectronics, Institute of Semiconductors, Chinese Academy of Sciences, Beijing 100083, China

Abstract Microwave photonics (MWP) is an interdisciplinary field that combines two different areas of microwave engineering and photonics. It has several key features by transferring signals between the optical domain and microwave domain, which leads to the advantages of broad operation bandwidth for generation, processing and distribution of microwave signals and high resolution for optical spectrum measurement. In this paper, we comprehensively review past and current status of MWP in China by introducing the representative works from most of the active MWP research groups. Future prospective is also discussed from the national strategy to key enabling technology that we have developed.

Keywords microwave photonics (MWP), integrated microwave photonics (IMWP), optical analog device and system, direct modulation laser, radio over fiber, phase stabilized analog optical link, optoelectronic oscillators (OEOs), microwave photonics filter (MPF), arbitrary waveform generation (AWG), optical phase locked looping (OPLL), microwave photonics front-ends (MWP-FE), optical vector network analyzer

1 Introduction

Microwave photonics (MWP) is a discipline that brings together the worlds of radiofrequency engineering and optoelectronics. Initially focused towards defense applications, has recently expanded to address a considerable number of civil applications: cellular, wireless and satellite communications, distributed antenna systems, sensing, medical imaging, etc [1 – 3]. Very recently, 5G mobile communications are targeted for 2020 and will need to meet very high demands: 1000-fold gain in capacity, connections from 100 billion devices, up to 10 Gb/s per user. MWP is considered one of the key enabling technology, which will be used to break the operation bandwidth limitation of pure microwave techniques.

MWP devices and systems have been used to realize different functionalities with unique performance that could not been realized using pure electronics techniques [4 – 6]. The general functionalities that have been realized and kept in investigation include microwave photonics filters (MPFs), optoelectronic oscillators (OEOs), arbitrary waveform generation (AWG), frequency mixing (FMIX), optically assisted analog to digital conversion (ADC), instantaneous frequency multiplication (IFM), tunable true time delay (TTD), tunable phase shifting (TPS), optical phase locked looping (OPLL), MWP front-ends (MWP-FE) and optical beamforming networks (OBFN).

MWP has been rapidly developed for more than 20 years, MWP systems and links have relied almost exclusively on discrete optoelectronic devices and standard optical fibers and fiber-based components. These configurations are bulky, expensive, power-consuming and lack flexibility. Emerging applications scenarios which will be a major driving force will require size, weight and power consumption (SWaP) reduction, reconfigurability and flexibility. Meeting these stringent requirements is only possible by developing integrated microwave photonics (IMWP) technology [7] and designing generic architectures that can be reconfigured via software-defined networking (SDN) techniques. There are several platforms that have been frequently used to demonstrate IMWP functionalities: indium phosphide (InP), silica planar lightwave circuits (PLCs), silicon-on-insulator (SOI), Si_3N_4/SiO_2, (TriPleX^{TM}) waveguide technology and $LiNbO_3$. Each technology has specific strengths but integration in single platform without sacrificing an overall system performance has not been achieved. In the near future, we have to identify the most suitable material platform which is compatible with generic fabrication models and the achievable performance should be compatible with present and future radio standards, such as the linearity, noise figure and dynamic range. In addition, another big challenge is that radio frequency (RF)/electronic/photonic components and subsystems needed to be integrated in a single platform.

Received February 24, 2016; accepted March 2, 2016

E-mails: ml@semi.ac.cn, nhzhu@semi.ac.cn

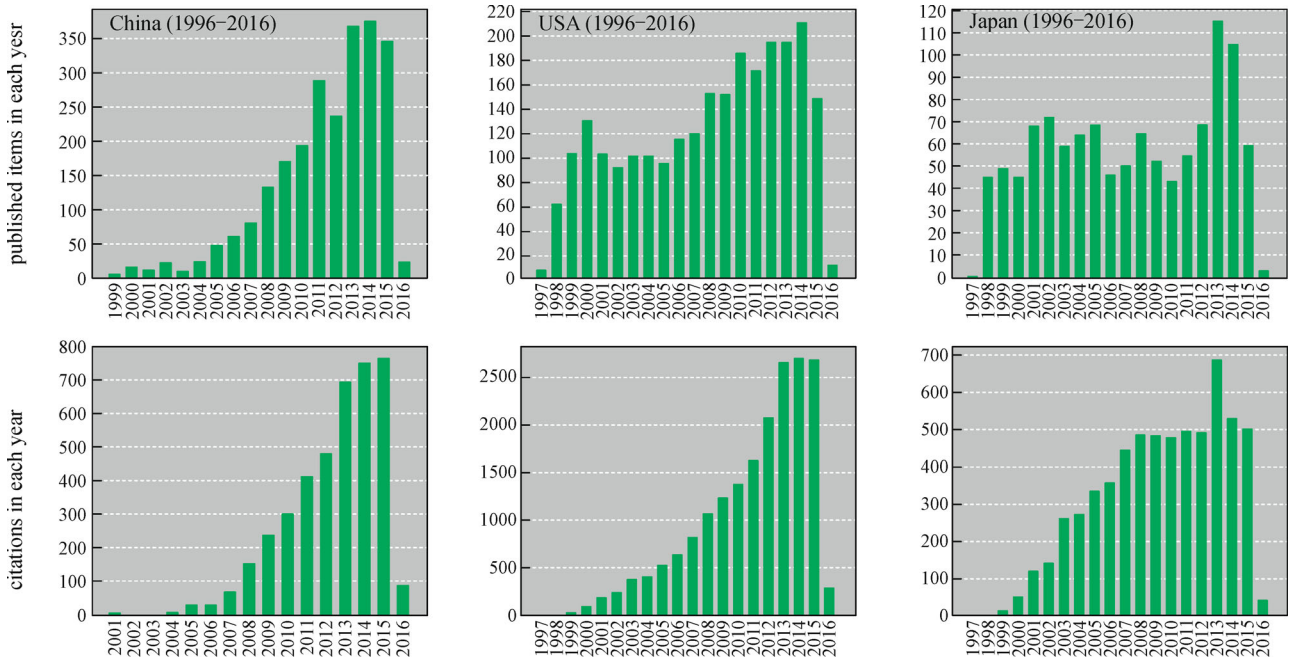

Fig. 1 Publications and citations records in the MWP topic of China, USA and Japan in the past 20 years (Data: from Web of Sciences)

As shown in Fig. 1, in the past 20 years, MWP technology has been widely investigated and the number of publications is kept increasing rapidly. The publication number on the topic of MWP from China has become the top one since 2009. Moreover, the increasing rate is kept much higher than the other countries. The total publication number in the past 20 years is approaching to the one of USA, as shown in Fig. 2. However, the average citation of each publication is only about 1.67, which is much lower than the other countries. It means that the quality of the publications from China should be largely improved. From 10 years ago, China started to support the development of MWP devices and system, as shown in Table 1. Based on the supporting of these funding, we have developed many key enabling technologies, in the meantime, the total publication number is increased rapidly year by year.

As shown in Table 1, two major "973" projects were funded by the Chinese Ministry of Science and Technology in 2012, simultaneously. One of the two "973" projects is entitled with basic research on MWP devices and integrated systems for broadband ubiquitous access, which is also named by another simplified name of Intelligent Radio Over Fiber (IROF). This "973" project's principal investigator is Prof. Yuefeng Ji from Beijing University of Posts and Telecommunications (BUPT), and totally 10 teams from different research organizations have been involved into this project such as Institute of Semiconductors, Chinese Academy of Sciences (IOS-CAS) and Tsinghua University etc. The main goals of this project are to reveal the mechanism behind efficient conversion between lightwave and microwave, to develop the fine

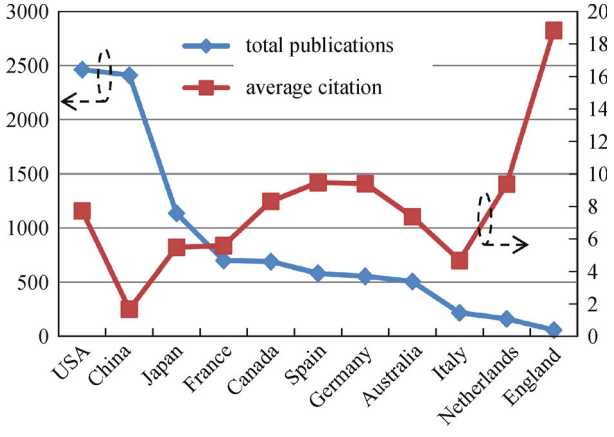

Fig. 2 Total publications and average citation of each publication of the active countries (Data: from Web of Sciences)

MWP signal processing techniques, and to derive the coordinated system model in a distributed network architecture. Several impressive results have been demonstrated experimentally, such as 24 GHz directly modulation laser [8] and 60 GHz integrated microwave photonic modulation chip.

The other "973" project is entitled with basic research on MWP for broadband and large dynamic-range millimeter wave devices and applications. The PI is Prof. Xiaoping Zheng from Tsinghua University, totally 7 universities in China have been involved into this project, such as Peking University, Shanghai Jiao Tong University (SJTU) and Beihang University. The main goals of this project are to

Table 1 Selected funded major projects on MWP in the past few years

year	type	research topics	principle investigator (PI)
2004	863	key technology of 10 Gb/s laser module for optical communications	Ninghua Zhu (IOS-CAS)
2007	863	key technology of integrated microwave photonic phase shifter based on SOI/PDLC	Weiyou Chen (Jilin Univ.)
2007	863	study on high speed MWP electro-optic modulator based on novel polymer materials	Xiaogong Wang (Tsinghua Univ.)
2009	863	high-speed linear modulated laser and transceiver module for radio over fiber	Liang Xie (IOS-CAS)
2009	863	research on the key technology of microwave photonic detection based on optical and wireless convergence	Xiaoxia Zhang (UESTC)
2011	863	photonic integration technology and system application	Ninghua Zhu (IOS-CAS)
2011	973	ultra high speed and low power photonic integrated circuits technology for information processing	Jianping Chen (SJTU)
2012	973	basic research on MWP for broadband and large dynamic-range millimeter wave devices and application	Xiaoping Zheng (Tsinghua Univ.)
2012	973	basic research on MWP devices and integrated systems for broadband ubiquitous access	Yuefeng Ji (BUPT)

investigate the fundamental theory and key enabling technologies for millimeter wave devices and applications based on MWP technology, in which the time-bandwidth product is targeted to be improved with three orders. Up to now, some impressive results have been achieved, such as the spectrum manipulating technique in the optical domain for its applications in MWP links and devices [9,10], and the phase error detection and phase noise (PN) compensation techniques in photonic microwave dissemination system [11].

In this review paper, we will first introduce the recent advances in MWP devices in Section 2, and then system-based works will be described in Section 3. Finally, future prospective will be discussed and conclusion will be made in Section 4.

2 Key MWP devices

MWP devices is related to those devices that is specially used in MWP system, as shown in Table 2. Some of them are similar to microwave and optical devices, such as broadband linear modulators and photodetectors (PDs). However, there still exist some devices that are designed and fabricated based on MWP techniques, such as directly modulation laser, OEOs and MPFs. In this section, we will introduce some exciting progresses on the MWP devices.

IOS-CAS is one of the leading optoelectronics research organizations in China with a State Key Lab on Integrated Optoelectronics, a national engineering research center for optoelectronic devices and an advanced optoelectronic devices packaging platform. In IOS-CAS, several groups are working on MWP from integrated chips, modules to application system. Among them, the microwave optoelectronics research lab is working on not only IMWP devices and modules such as directly modulation laser and optical analog signal processor, but also application systems such as phase stable MWP link and true time-delay beamforming system.

In 2012, Prof. Zhu and Prof. Wang's group from IOS-CAS reported a distributed feedback (DFB) laser with 24 GHz bandwidth. The packaged prototype devices and

Table 2 Comparison of microwave, optical and MWP devices

functionality	microwave devices	optical devices	MWP devices
source	oscillator	laser	direct modulation laser/OEO
modulation	modulator	electric absorber/$LiNO_3$	broadband linear modulator
waveguide	RF cable	optical fiber	RF cable and optical fiber
detection	detector	PD	broadband linear PD
amplification	RF amplifier	EDFA/SOA	RF and optical amplifier
filter	RF filter	optical filter	MWP filter

Notes: EDFA: erbium-doped fiber amplifier; SOA: semiconductor optical amplifier

bandwidth characteristics of the 24 GHz analog direct modulation laser is shown in Fig. 3 [8]. In addition, based on a distributed feedback semiconductor optical amplifier (DFB-SOA), a widely tunable single passband MPF is proposed and experimentally demonstrated. By tuning the central wavelength of DFB-SOA base filter, a single-channel MPF with frequency tuning range from 5 to 35 GHz is obtained [12].

Figure 4 gives the experimental setup for microwave generation using an electro-absorption modulator (EAM) integrated in between two DFB lasers [13]. In this scheme, the wavelengths of the DFB lasers are tuned by adjusting their bias currents. The light beams from both DFB lasers are injected into the EAM and mixed with each other to generate microwave signal. Figure 5 shows the optical and electrical spectra. In Fig. 5(a), four-wave mixing effect can still be observed when the optical wavelength difference is over 30 GHz due to strong optical coupling between the two lasers. From Fig. 5(b), it can be seen that a sharp peak at the beat frequency has a 24-dB signal noise ratio. The frequency of the generated microwave signal can be tuned by changing the bias currents of the DFB lasers.

As shown in Fig. 6, Prof. Zhao from IOS-CAS fabricated three-section amplified feedback lasers (AFL) on InP substrate. By controlling the currents injected into the three sections of the AFL, various working states including single mode, dual mode, periodic oscillation and chaotic states have been demonstrated [14]. Dual-mode AFL has also been employed in OEO structures, simultaneously functioning as a laser source, active photonic filter, and modulator [15].

Prof. Huang's group in IOS-CAS proposed to use integrated semiconductor twin-microdisk laser for microwave signal generation under mutually optical injection through a connected optical waveguide with the mode wavelength intervals adjusted by injection currents [16]. Dynamical characteristics are also investigated for square resonator microlasers subject to optical injection, the microwave signals are obtained from the electrode of the microlasers subject to optical injection related to the oscillation of carrier density in the active region as shown in Fig. 7 [17].

There are several groups from Tsinghua University actively working in the field of IMWP devices. Prof. Chen proposed a full-band (from L-band to W-band) RF photonic frontend, which is based on the integrated high Q, large processing range tunable signal processor as presented in Fig. 8(a). Based on this RF photonic frontend, the RF signal would be up-converted to optical domain and processed by the full-band signal processor to obtain the desired signal band. As shown in Fig. 8(b), the spurious free dynamic range (SFDR) of the frontend measured has been presented, at frequency from 1 to 65 GHz. This is the first proposed RF photonic frontend, which could work from L-band to W-band and this frontend will likely have extensive applications in either the wireless communications or radar communications field [18,19].

Prof. Luo's group from Tsinghua University realized an uni-travelling-carrier photodiodes (UTC-PDs), in which the photon-absorption is mainly in the p-layers and only electrons diffusion and drift are needed, have exhibited high speed and saturation optical power performance which are important for high performance microwave photonic links. As shown in Fig. 9, the 3-dB bandwidth reaches over 40 GHz for the first time in such high responsivity mesa structure PDs, with a measured photocurrent over 47 mA at 30 GHz at 1-dB compression point [20].

In addition, as shown in Fig. 10, an integrated dual wavelength laser diode (LD) is fabricated for optical generation of millimeter-wave (MMW) carrier with high spectral purity [21]. The integrated device consists of two DFB lasers and one Y-branch coupler monolithically integrated on the same AlGaInAs multiple quantum well (MQW) active layer. A 42 GHz mm-wave carrier is generated from a 5.25 GHz modulation signal, corresponding to eight-fold frequency multiplication. The measured PN performance of the 42 GHz mm-wave carrier is as low as –94.6 dBc/Hz at 10 kHz offset.

Several groups from Huazhong University of Science

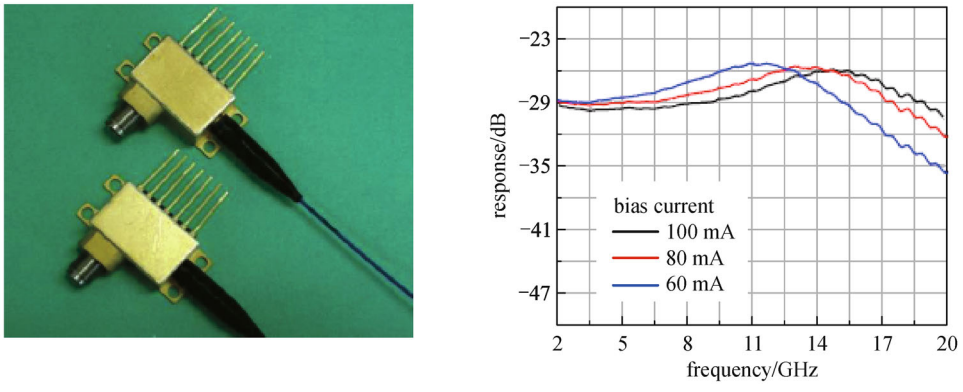

Fig. 3 Prototype devices and bandwidth characteristics of the 24 GHz analog direct modulation laser [8]

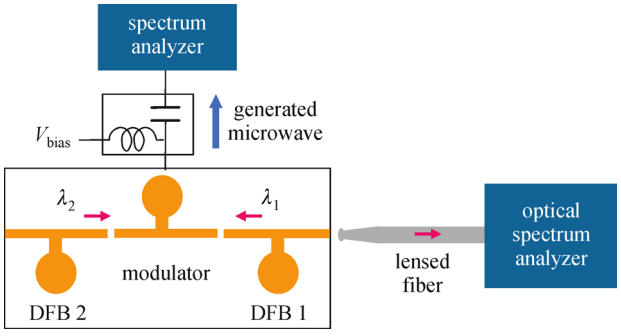

Fig. 4 Experimental setup for microwave signal generation using an EAM integrated in between two DFB lasers [13]

and Technology (HUST) are also working on IMWP devices mainly based on passive/silicon photonics devices. Prof. Wang's group at Wuhan National Laboratory for Optoelectronics (WNLO) realized an ultra-high peak rejection notch MPF using silicon waveguides, silicon microring resonators, and silicon photonic crystal nano-cavities as shown in Fig. 11 [22].

In 2010, Prof. Zhang from WNLO in HUST declared to implement an MPF with the highest Q factor of 3338. In 2013, this research group has demonstrated a notch MPF based on cascaded SOI microring resonators (MRRs) with different radii [23]. As shown in Fig. 12, the tuning of input laser wavelength is not necessary and the frequency tunability is continuous. They demonstrated a central frequency tuning range from 19 to 40 GHz, and a wide bandwidth tuning range from 5.5 to 17.5 GHz.

A few researchers from SJTU are working on silicon photonics based IMWP devices such as tunable delay line and optical filter for microwave signal generation. From Prof. Chen's group, as shown in Fig. 13(a), they proposed an N-bit reconfigurable optical true time delay line (RTTDL) using cascaded optical switches and waveguide delay lines [24]. The optical delay can be varied by reconfiguring the switches to provide different optical paths for the light to pass through. The switch is made of a 2×2 Mach-Zehnder interferometer (MZI) with a PIN diode integrated in one arm to enable fast electrical tuning. Figure 13(b) shows the microscope image of the fabricated 7-bit RTTDL. The chip size is 7 mm × 1.5 mm. Figure 13 (c) presents the images of the chip after home package. The chip is wire-bonded to a print circuit board and coupled with a fiber array. Figure 13(d) shows the output pulses after various delays. The delay is relative to the reference pulse which passes through the shortest path. The delay increases from 10 to 640 ps when each stage is switched to the longer waveguide. The delay reaches to the maximum of 1.27 ns when all longer waveguides are selected. Therefore, the RTTDL can provide 128 delays with a resolution of 10 ps. The RTTDL has time delay invariance to RF frequency. Figure 13(e) shows the phase of the received RF signal as a function of frequency when the carrier light passes through the shortest and longest paths. The phases changes linearly with the RF frequency. The time delay is given by the phase derivative to the angular frequency. The relative delay between the longest and shortest path is 1.3 ps, agreed with the pulse transmission measurement.

Researchers from Prof. Su's group in SJTU demonstrated tunable microwave photonic filtering and MMW signal generation with a silicon photonic device termed as self-coupled micro-resonator (SCMR) [25]. By tuning the resonance notch interval of an SCMR with an interferometric central coupler and using the through port as the output, they have demonstrated a continuously tunable microwave photonic notch filter with a high rejection ratio over 25 dB and a wide tuning range over 20 GHz. The micrograph of the fabricated device and the measured frequency responses are shown in Fig. 14(a). While if using the drop port of the device as shown in Fig. 14(b), with an input of optical frequency comb (OFC) spaced by ~9.7 GHz, photonic generations of ~39-GHz and ~29-GHz MMW signals can be achieved by thermally tuning the passband spacing.

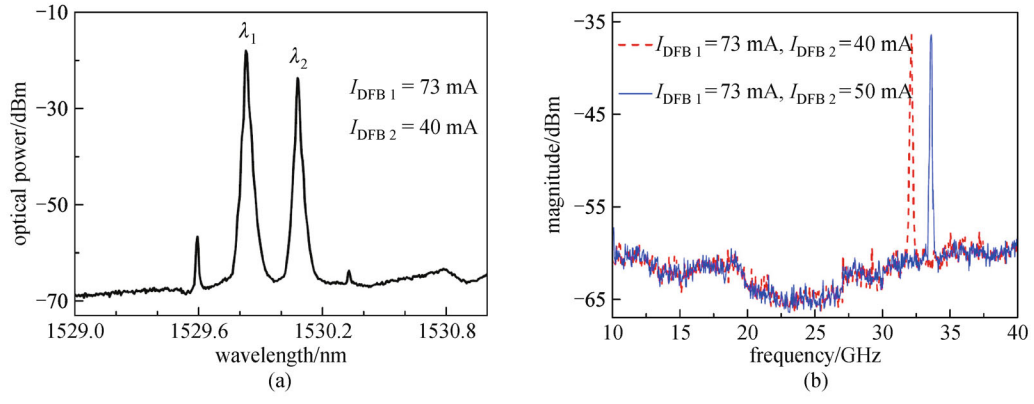

Fig. 5 (a) Optical spectrum and (b) corresponding electrical spectrum (dashed line). The electrical spectrum after adjusting the bias current of the DFB laser 2 is also included [13]

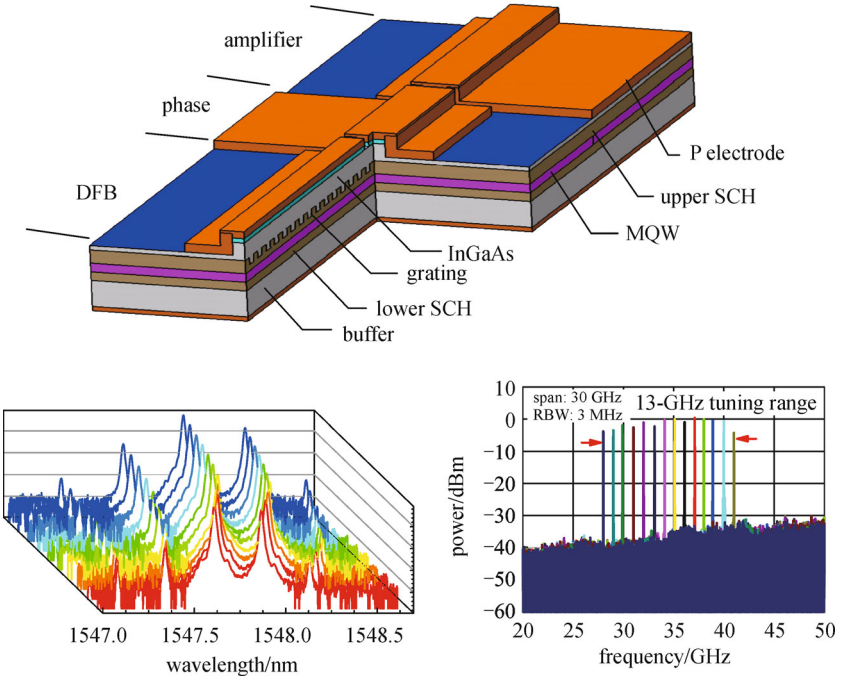

Fig. 6 AFL (upper) consisting of a DFB, a phase and an amplifier section; dual-mode state of an AFL (lower left); tunable output from an AFL-based OEO (lower right). SCH: separate confinement heterostructure; MQW: multiple quantum well [14,15]

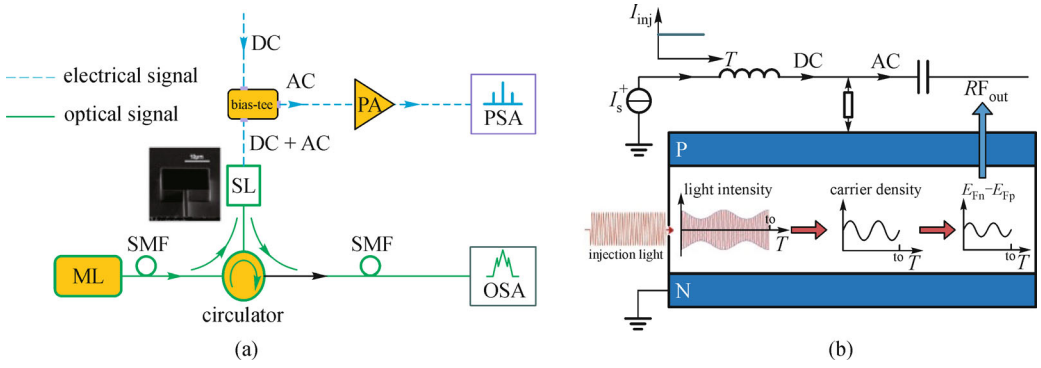

Fig. 7 (a) Schematic of the experiment system setup. ML: master laser; SL: slave laser, i.e., microsquare laser; PA: power amplifier; PSA: PSA series spectrum analyzer; SMF: single-mode fiber; OSA: optical spectrum analyzer; (b) principle schematic of photonic generated microwave inside the microcavity laser. T: time; $E_{Fn} - E_{Fp}$: the difference of the Fermi levels [16,17]

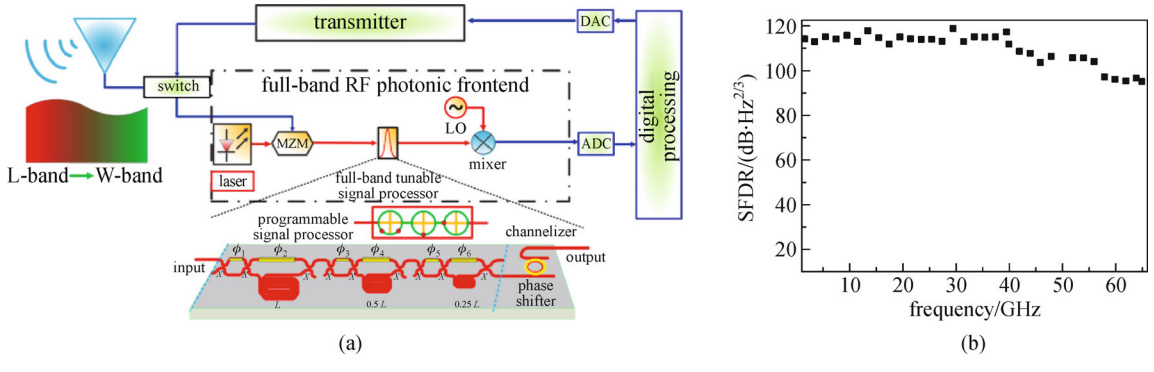

Fig. 8 Full-band RF photonic frontend. (a) Schematic diagram of the full-band RF photonic frontend based on the integrated full-band tunable signal processor; (b) measured SFDR of the frontend from L-band to U-band, covering from 1 to 65 GHz [18,19]

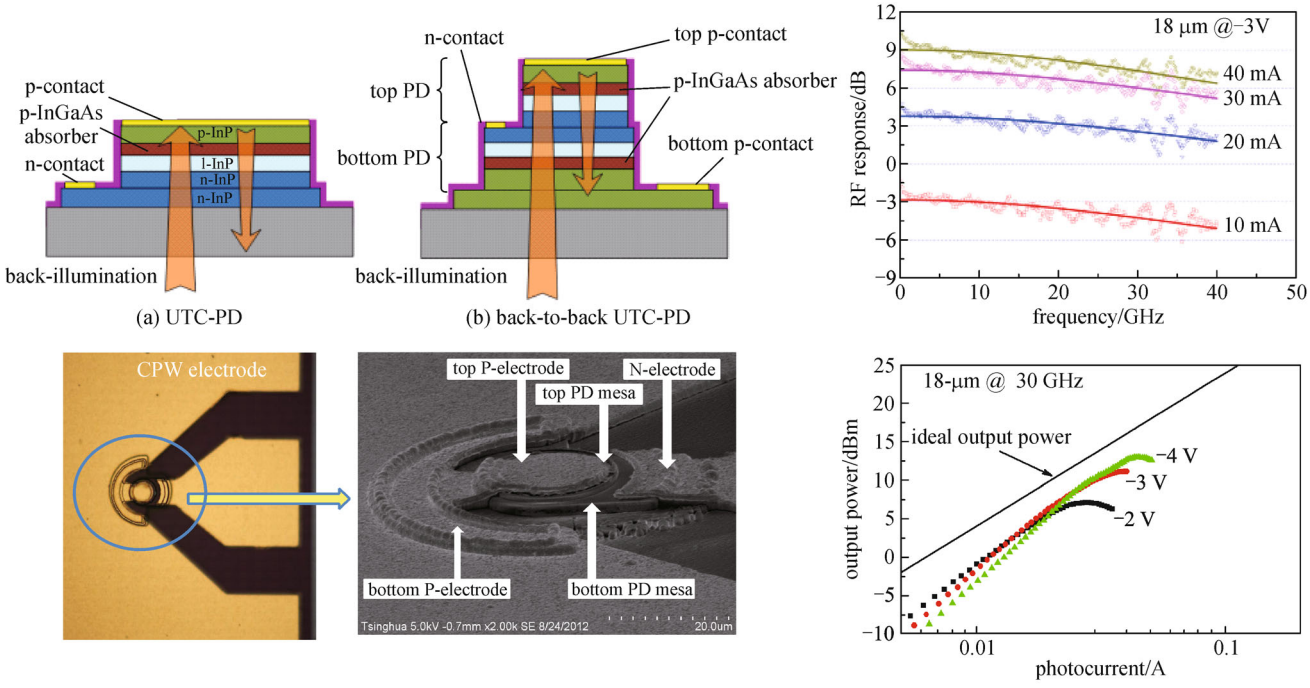

Fig. 9 High responsivity, high speed and high power integrated photodiodes based on back-to-back stacked UTC structure. CPW: coplanar waveguide [20]

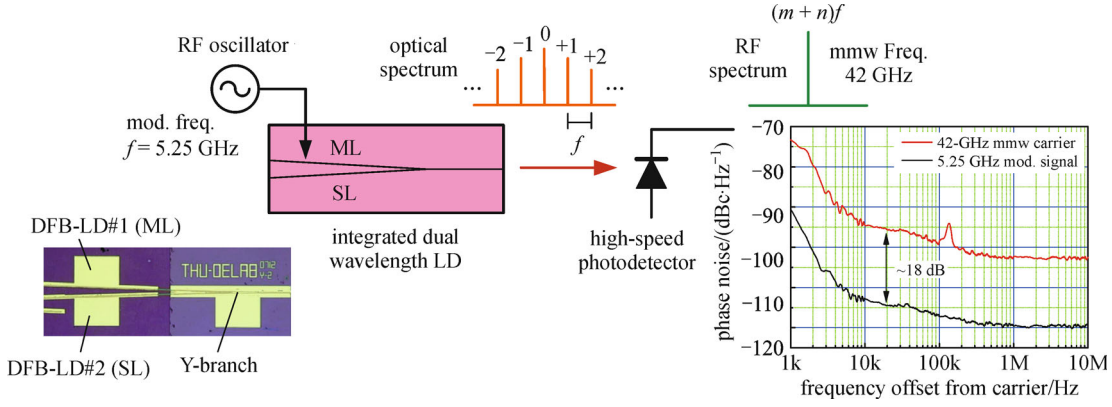

Fig. 10 High spectral purity mm-wave carrier generation by modulation sideband injection locking of integrated dual wavelength laser diode (LD) [21]. ML: master laser; SL: slave laser

Besides of the fabrication of IMWP devices, high-speed optical modulators and PDs are basic components in MWP links. High-frequency responses of these optoelectronic devices are critical to the wideband electrical-to-optical or optical-to-electrical signal conversion. The conventional swept frequency method needs a pair of modulator and PD, and it relies on de-embedding the frequency response of the assisted devices except the device under test (DUT) [26], since the measured results are always contributed by both the modulator and the PD in the setup. Recently, Zhang and Liu at University of Electronic Science and Technology of China (UESTC) proposed a novel frequency-shifted heterodyne method and demonstrated for the self-calibrated high-frequency response measurements of Mach-Zehnder modulators (MZMs) [27,28], phase modulators (PMs) [29,30] and PDs [31]. The method is illustrated in Fig. 15 within one setup. The MZM, PM and PD can be independently self-calibrated measured at different modulation frequencies through carefully setting the frequency relationship between the driving microwave signals. The method enables high-resolution self-calibrated frequency response measurement

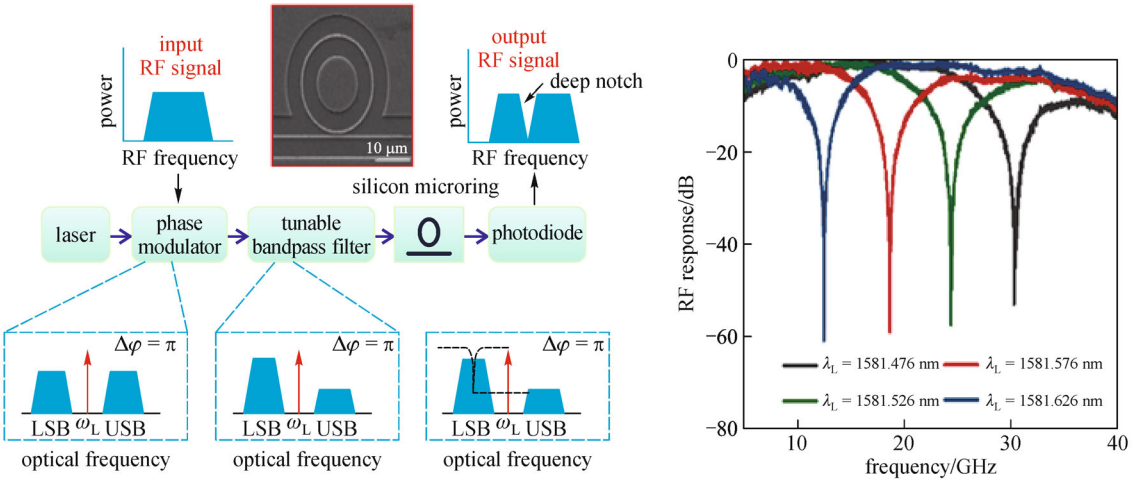

Fig. 11 Concept and principle of the notch MPF with ultra-high peak rejection and the measured RF responses of tunable ultra-high peak rejection MPF under different optical carrier wavelengths. LSB: lower sideband; USB: upper sideband [22]

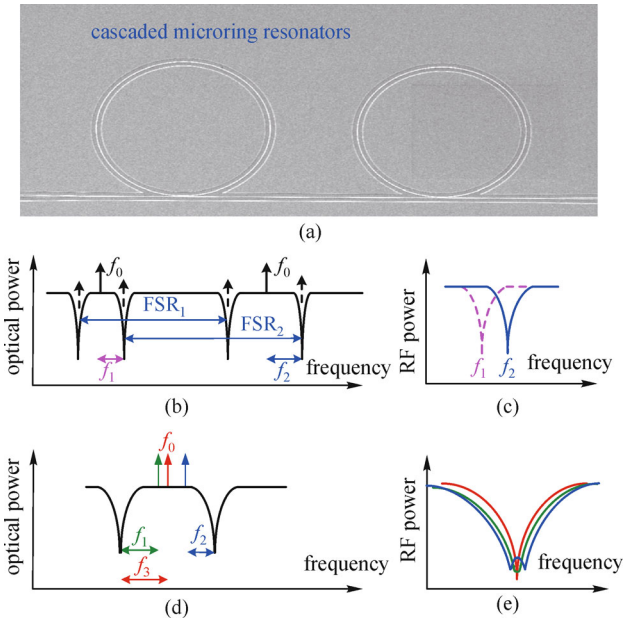

Fig. 12 (a) Scanning electron microscope (SEM) images of the cascaded microring resonators (CMRRs); (b) and (c) tunability of central frequency of the MPF; (d) and (e) tunability of bandwidth of the MPF. FSR: free spectral range [23]

of MZMs, PMs and PDs, and eliminates the need to correct the influence from other assistant devices in the measurement, which largely simplifies the high-frequency characterization of high-speed optoelectronic devices.

3 MWP system

In the past few years, MWP subsystems towards practical applications have been demonstrated in China, such as programmable MPF, stable RF phase distribution, indoor building radio access network, OBFN and optical vector spectrum analyzer, which will be introduced simply as following.

Prof. Zheng from Tsinghua University has been working on the spectrum manipulating in the optical domain and its applications in MWP links and devices. Spectrum structures of microwave photonic links with dispersion [32] or nonlinearity from MZM [33,34] or EA [35], and their evolutions during the photo detection have been analyzed, and compensation techniques for fiber dispersion and nonlinearity for modulators have been proposed by

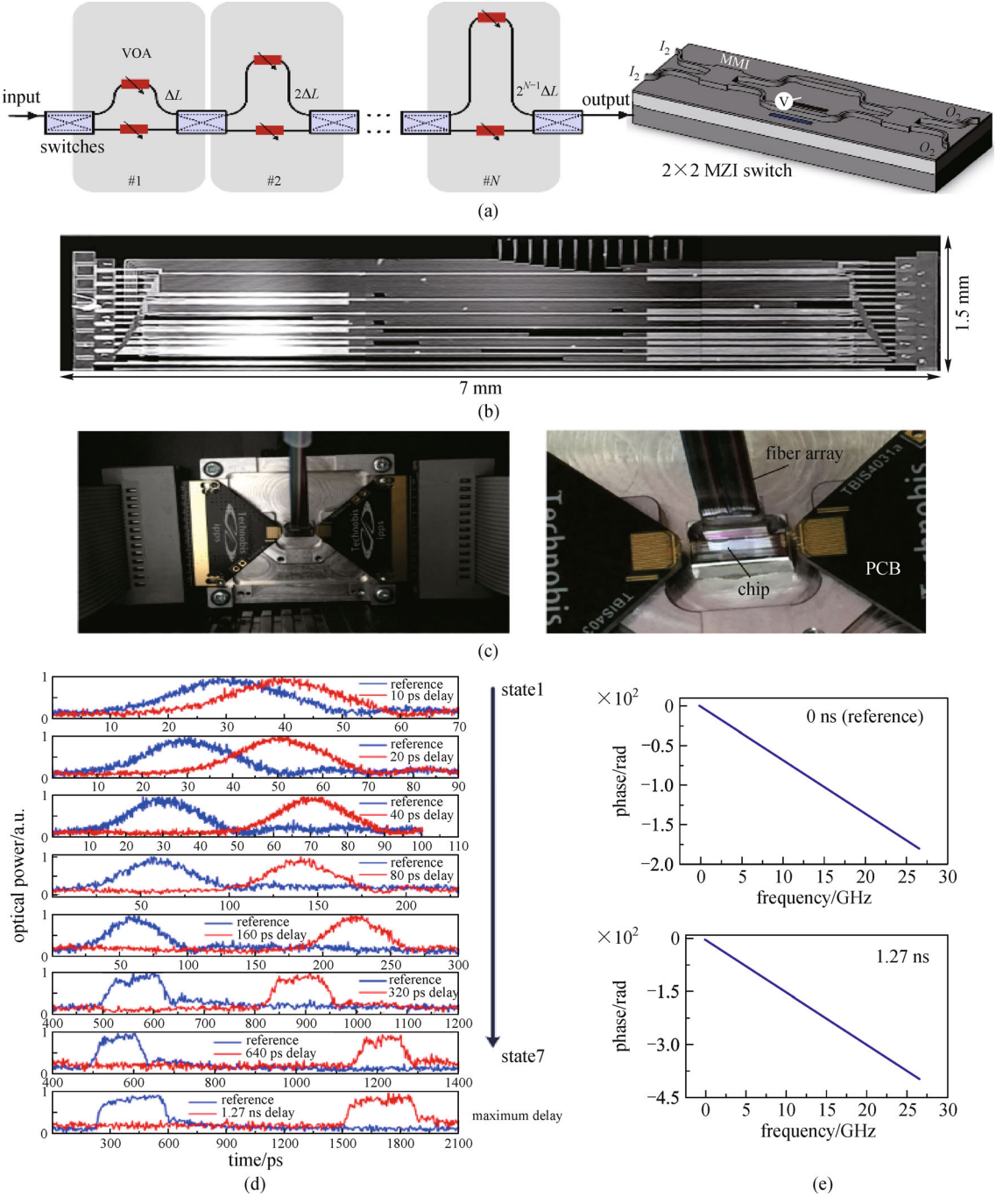

Fig. 13 (a) Schematic structure of the RTTDL. The switch is based on a 2×2 multimode interference (MMI); (b) optical microscope image of the fabricated chip; (c) optical photo of the package chip; (d) measured output pulses with 10 ps to 1.27 ns optical delays with respect to the reference pulse; (e) measured frequency responses of the unwrapped transmission phase for the minimum and the maximum delays [24]

manipulating optical spectrum with DPMZM [32] or spatial light modulator [33,37]. And FSDR of radio over fiber transmission links with commercial optical devices can be easily improved using these techniques to more than 122 dB·Hz$^{2/3}$ [32,34] for MZM based links and 115 dB·Hz$^{2/3}$[36] for EA based link with a frequency lower than 20 GHz, and to 107 dB·Hz$^{2/3}$[36] for MZM based link with 60 GHz frequency band. The technique for dispersion compensation is widely applied to enhance performances of other MWP subsystem. A high resolution time delay control is realized by the technique to add a quadratic optical phase shift and compensates the group velocity

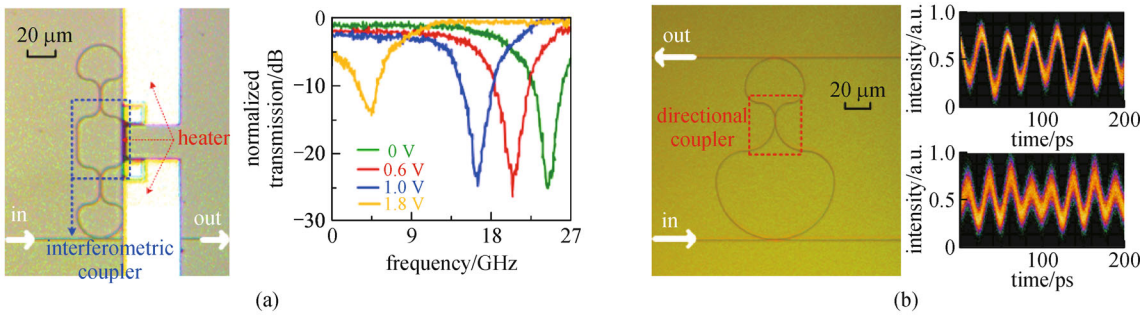

Fig. 14 (a) Micrograph of the fabricated SCMR and measured microwave frequency responses for varied applied DC voltages; (b) micrograph of the fabricated SCMR with its drop port as the output, and temporal waveforms of the generated 29-GHz / 39-GHz MMW signals [25]

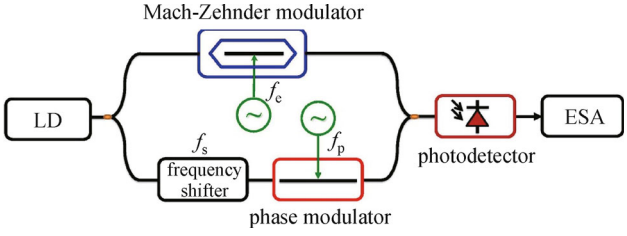

Fig. 15 Schematic diagram of the frequency-shifted heterodyne method within one setup. In the case of the Mach-Zehnder modulator (MZM) as DUT, the microwave frequency of MZM is set close to twice of that of PM. In the case of PM as DUT, the microwave frequency of PM is set close to twice of that of MZM. In the case of PD as DUT, the microwave frequency of MZM is set close to that of PM [29]. ESA: E series spectrum analyzer

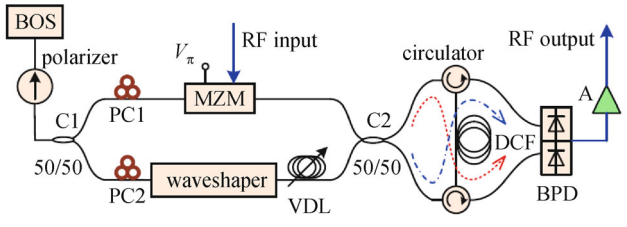

Fig. 16 Incoherent-BOS-based MPF features single-bandpass, widely tunable (0–20 GHz), arbitrary shape with Q value controllable. Followings show some figures to prove the abilities of the filter [41]. PC: polarization controller; BPD: balanced photodetector

dispersion (GVD) of the fiber simultaneously. A coarse tuning range of 1717 ps and a high resolution of 0.67 ps is achieved [37]. It is employed to suppress the dispersion induced PN in optically generated MMW and fiber transmission. An MMW PN amelioration of 12.63 dB at 10 kHz offset and 11.23 dB at 100 kHz offset is achieved in a 40 GHz, 25 km optical MMW link thanks to this technique [38]. Also, we realized dispersion free transmission of ultrawideband (UWB) over fiber under a different length of fiber [39].

In addition, Prof. Zheng is also working on the highly reconfigurable microwave photonic single-bandpass filter with complex continuous time impulse responses [40,41]. The filter is based on the so-called equivalent electrical slicing together with programmable optical spectrum processor [40]. The schematic diagram of the filter is shown in the figure [41]. The incoherent light from a incoherent broadband optical source (BOS) (e.g. erbium-doped fiber amplifier (EDFA) or light-emitting diode (LED)) is polarized and split into two branches via a 1 × 2 coupler (C1). One branch is modulated by the microwave input via a single-drive MZM biased at the minimum transport point, as shown in Fig. 16. The other branch is spectrum tailored via a WaveShaper which is a commercial programmable optical processor, and time delayed via a variable optical delay line (VDL). The two branches are then combined again in the same polarization via a 2 × 2 coupler (C2). The two outputs of C2 go through a dispersive element which is a length of dispersion-compensating fiber (DCF) in opposite directions via two circulators and differentially detected. WaveShaper acts as a programmable optical filter with arbitrary amplitude and phase responses. VDL is for tuning the central frequency of the filter. As shown in Figs. 17 and 18, the shape of MWP filter keeps unchanged when tuned from DC-20 GHz, and the highest Q value is 634. Additionally, a flat-top shape with lower Q value when tuned from DC-20 GHz has also been realized, as shown in Fig. 18.

Prof. Li and Prof. Feng from Jinan University are also working on MPFs. Prof. Feng's research is focused on the investigation of new microwave photonic signal processing techniques by using a Fourier-domain optical processor (FD-OP). She reported a series of FD-OP based microwave photonic signal processors that exploit the gain-bandwidth and reconfigurability advantages of photonics to overcome the limitations of conventional processors [42]. Prof. Li realized a MPF with an ultra-high Q value of 4895 utilizing cascaded optical-electrical

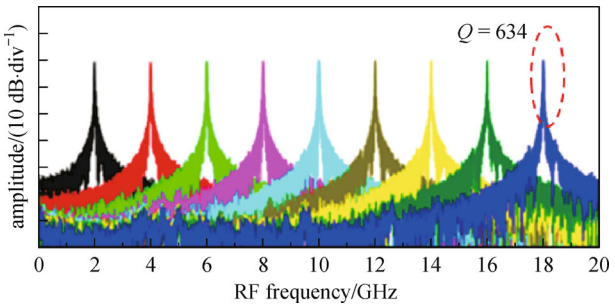

Fig. 17 Shape keeps unchanged when tuned from DC-20 GHz, and the highest Q value is 634 [41]

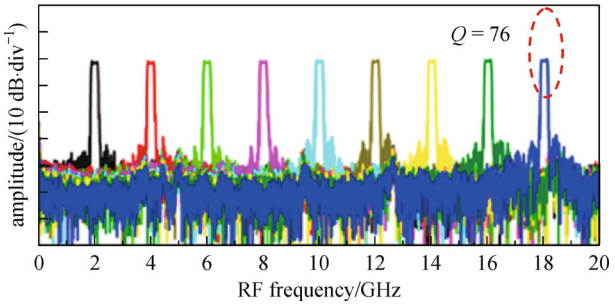

Fig. 18 Unchanged flat-top shape with lower Q value when tuned from DC-20 GHz [41]

feedback loops. As shown in Fig. 19, an infinite impulse response (IIR) filter with both optical and electronic signals in a feedback loop is proposed to overcome the problem of optical coherent interference. In addition, we improve the Q value of an IIR filter with two cascaded optical-electrical feedback loops, in which the Vernier effect can help to select the frequency components passing through both cascaded loops and therefore significantly increase the FSR of the filter. As a result, an highest reported Q value of 4895.31 is achieved for the proposed IIR filter [43]. In addition, the ability to vary the Q value of the proposed microwave photonic filter can be achieved by carefully adjusting loop lengths of the two cascaded filters, and the frequency response of the filter with a fixed Q can also be changed by tuning the bias of the MZMs in the two loops.

In order to meet the requirements for the development of three networks (telecommunication network, radio and television network, Internet), the radio and television network not only can provide voice, data and high-definition television and other cable services for the users, but also will provide Internet, mobile TV, mobile communications and other wireless services. In view of the above requirements, our research group mainly focuses on studying the architecture, system components and key technologies of the RF access system. Prof. Xin from BUPT has reported several significant works [44–47]. They realize a flexible scheduling and dynamic bandwidth allocation is realized by using orthogonal frequency division multiplexing (OFDM) subcarrier to carry multi service. In addition, the wireless/optical fiber integrated system with multi-users, long distance, and large capacity is realized via combining radio-over-fibre (ROF) with passive optical network (PON) technology, as shown in Fig. 20. Moreover, as shown in Fig. 21, a real-time video transmission platform based on 60 GHz technology is built, which can realize the 1 Gb/s high definition (HD) video transmission with free bit error rate, and realize the seamless integration of the optical fiber 25 km and wireless 10 m access. The radio passive optical network (RPON) access system, whose index has reached the international advanced level, has been considered as the promotion project by Shanxi Province Radio and Television Information Network Co., Ltd.

In photonic microwave dissemination system, a novel phase error detection and PN compensation scheme have been proposed by Prof. Dong from SJTU [48–51]. As shown in Fig. 22, the former contains an optic heterodyne beating and an electrical heterodyne beating, while the latter includes an electrical phase locked loop (PLL) and an acousto-optic frequency shifter (AOFS). Based on the dual-heterodyne phase error transfer (DHPT) and fast phase corrections scheme, we have achieved highly stable remote distribution microwave signal of 10 GHz over 100 km, 20 GHz over 100 km, 100 GHz over 60 km spooled optic fiber, and 1 THz over 42 km dark optic fiber respectively. Long-term stability of microwave signal dissemination is achieved and shown in Fig. 23.

Prof. Sun from HUST published some impressive works on the generation, modulation and measurement of microwave signal. They demonstrate a photonic approach to simultaneously realize a frequency-multiplied and phase-shifted microwave signal based on the birefringence effects in the high nonlinear fiber (HNLF) [52]. The phase shift caused by asymmetric variations in refractive indexes of fiber between two orthogonal polarization states is introduced into two coherent harmonics which will be beaten in the PD. A microwave signal at doubled- or quadrupled-frequency with a full 2π phase shift is obtained over a frequency range from 10 to 30 GHz. In addition, they realized a tunable optical carrier-to-sideband ratio (OCSR) by introducing two RF signals with phase difference to drive an MZM. Stimulated Brillouin scattering (SBS) is adopted to remove the undesirable sideband, converting double sideband (DSB) to single sideband (SSB) [53]. Wide ranges of OCSR from −23 to 44 dB and −21 to 44 dB are obtained for the DSB and SSB modulation. Moreover, they experimentally demonstrate a novel approach for microwave frequency measurement utilizing birefringence effect in the HNLF [54]. As shown in Fig. 24, a frequency measurement range of 2.5–30 GHz with a measurement error within 0.5 GHz is achieved except 1–2.5 GHz and 16–17.5 GHz.

Prof. Chi and his colleagues in Zhejiang University, Hangzhou focus on the photonic realization of compres-

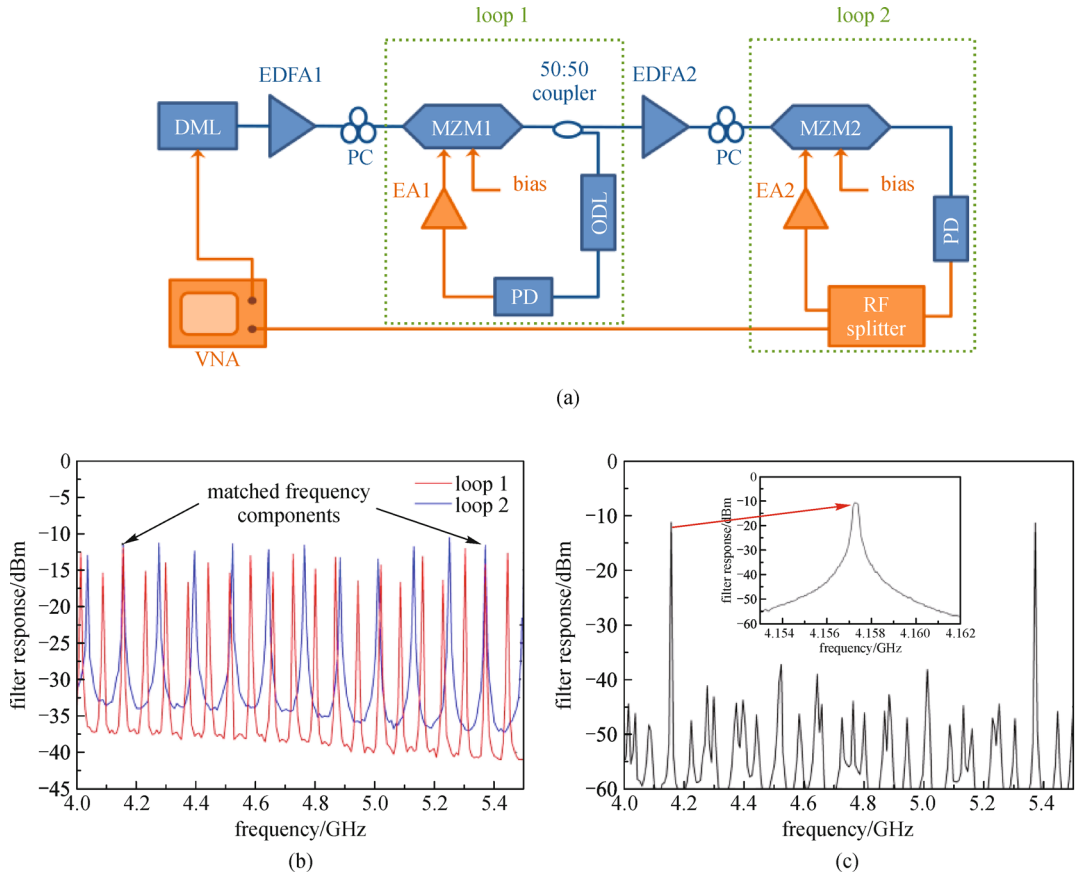

Fig. 19 (a) Experimental setup; (b) frequency response of the IIR filters with one loop; (c) frequency response of the IIR filter with two cascaded loops [43]. DML: directly modulated laser; VNA: vector network analyzer; EA: electrical amplifier; PD: photo detector; ODL: optical delay line

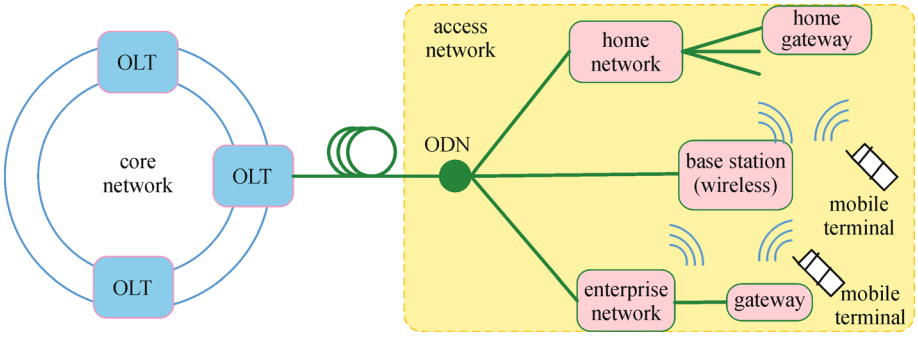

Fig. 20 Structure diagram for integrated access network. OLT: optical line terminal; ODN: optical distribution network [45–47]

sive sensing (CS) for the acquisition of wideband sparse signals in recent years [55 – 61]. They have proposed and investigated some approaches to optically realize the functions which are necessary for the CS, such as random mixing and integration [55 – 59]. To largely decrease the required sampling rate, they have proposed a sub-Nyquist sampled photonic analog-to-digital converter based on the techniques of photonic time stretch and CS [60,61], which is shown in Fig. 25.

Prof. Xu from BUPT has proposed a satellite repeater architecture which consists of multiple paths to support repeating signals among the C, Ku, K and Ka bands [62,63], as shown in Fig. 26. Note that all the paths share a common local oscillators (LOs) generation module and an optical switch matrix that dramatically saves LOs and space on the satellite. The whole system can be divided into three sections, the multi-band LOs generation section, the band to band conversion section and the optical cross-

Fig. 21 60 GHz HD video real-time optical access platform

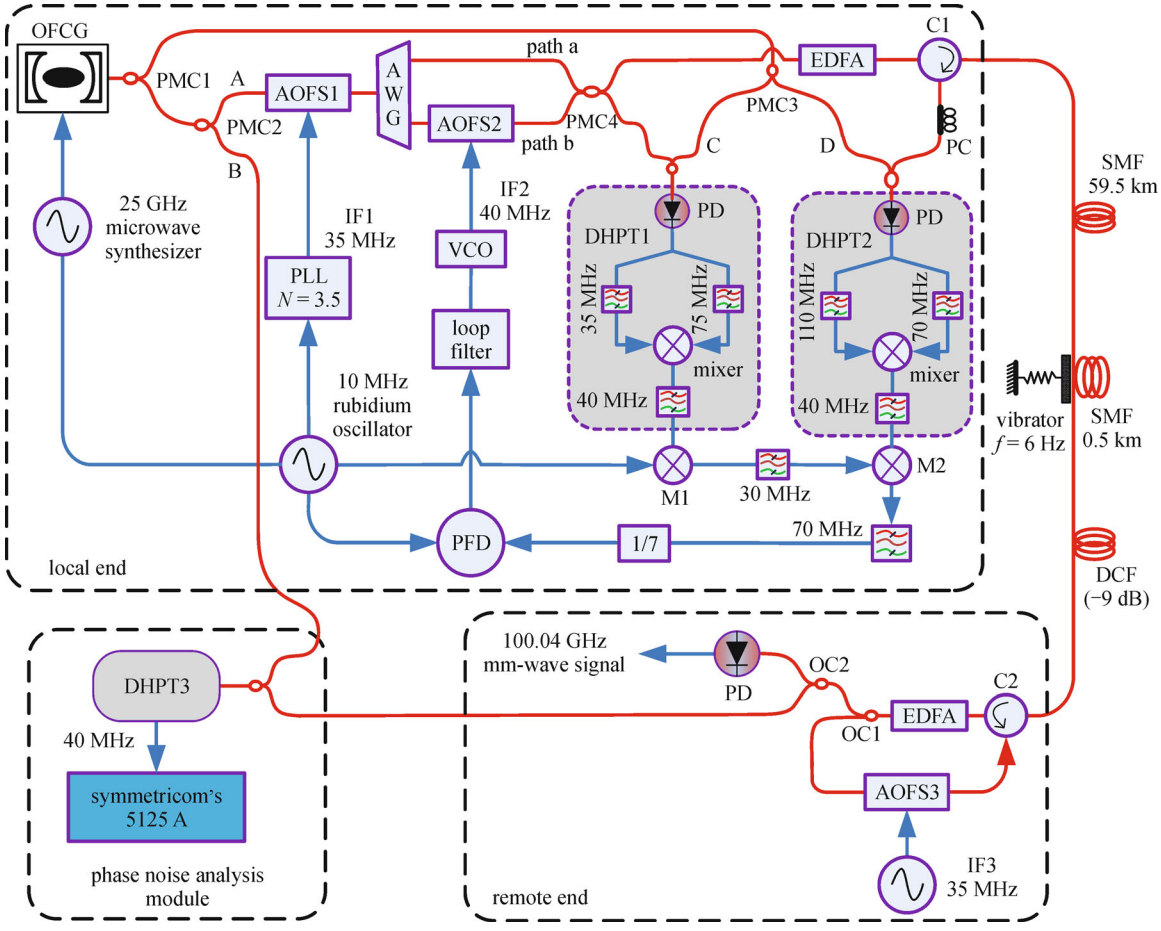

Fig. 22 Experimental setup for stable dissemination millimeter-wave signal system [48–51]. OFCG: optical frequency comb generator; PMC: polarization maintaining coupler; AWG: arrayed waveguide grating

connect section. In particular, these three sections can be compatible with each other since all their functions are implemented in optical domain. Consequently, this concept of microwave photonic repeater is very suitable for transparent and broadband telecom missions. Besides, such microwave photonic system with parallel structure offers high scalability, thus it can be upgraded to large scale with the number of channels. In the future, once integrated into a single chip, this concept will bring the current all-microwave repeaters to a new era with unprecedented performance improvement.

The MWP group from Beihang University is at a unique position to investigate and pursue applications of the microwave photonic technologies to bridge the gap between the microwave and photonic worlds. In the past few years, their focus has been on microwave photonic technologies based on OFCs, as shown in Fig. 27. Through generating versatile and tunable optical combs by electrical-to-optical (EO) modulation [64], RF waveform generation and spectrum measurement over a wide frequency range are demonstrated [65]. Based on innovative cavity structures that enable wavelength-, polarization-multiplexing in ultrafast fiber lasers, multiple OFCs could be generated from a single optical cavity. Due to the correlation between such generated comb pairs that suppresses the common-mode noises, asynchronous opti-

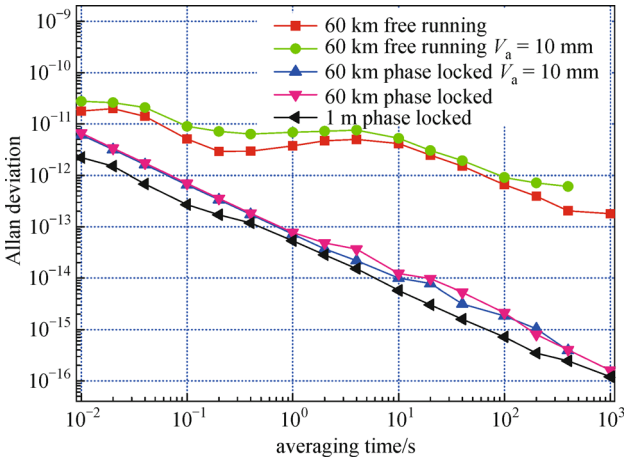

Fig. 23 Allan deviation of remote distribution system [48–51]

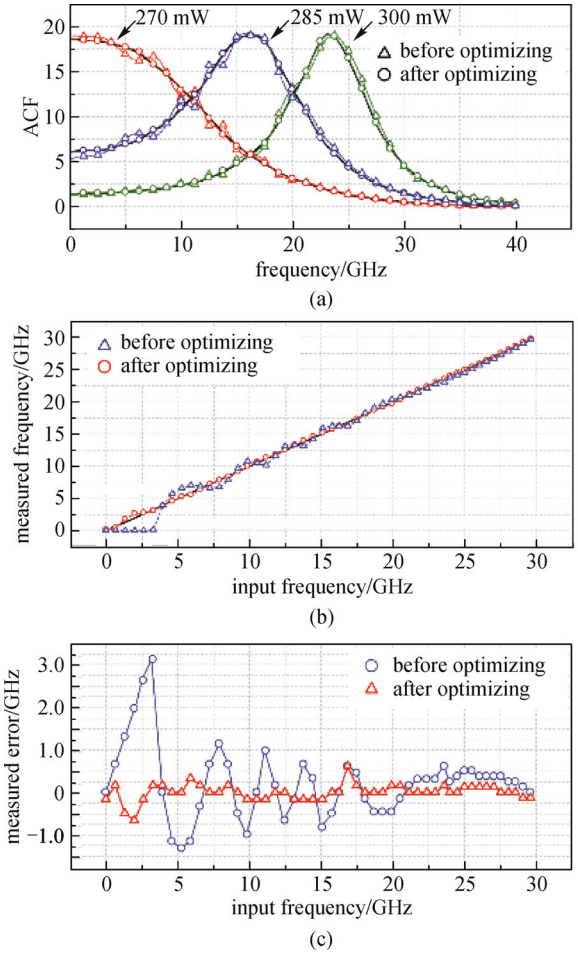

Fig. 24 (a) Measured and theoretical (solid line) amplitude comparison function (ACF) when P_m= 270, 285 and 300 mW; (b) measured microwave frequencies when the input microwave frequency is tuned from 0 to 30 GHz; (c) distribution of the measurement errors [54]

cal sampling with high bandwidths could be realized [66], which would enable fast, high-resolution characterization and manipulations of, up-to-THz, microwave signals with many potential applications in sight.

Recently, Prof. Yi et al. in SJTU have solved the problems and demonstrated a rectangular MPF based on SBS effect in optical fiber [67 – 71] and offering tunability on bandwidth, central frequency and selectivity as shown in Fig. 28. A sweeping-pump multi-stage configuration with feedback control is implemented to achieve the rectangular MPF with high selectivity. The obtained 20 dB shape factor is as low as 1.056, which is the best reported result for MPF in ~GHz bandwidth. Furthermore, they solved the polarization-dependent SBS gain issue and realized a polarization-independent MPF. The SBS noise is reduced by adopting a multi-stage configuration to limit the gain at each stage. Finally, the filter selectivity for a four-stage configuration is as high as 57 dB for a 2.1 GHz bandwidth. In this case, the signal-to-noise ratio penalty is only 2.6 dB for a 4 Gbit/s OFDM signal in quadrature phase shifted keying (QPSK) format.

Emergency services, when large-capacity long-distance optical cables are cut during natural disasters such as earthquake and tsunami, as well as mobile backhauling between wireless macro stations, require wireless links with both large transmission capacity and long transmission distance. Broadband mm-wave generation based on photonic techniques can overcome the insufficient bandwidth of commercially available electrical components and promote the seamless integration of wireless and fiber-optic networks. The research group from Fudan University has accomplished a series of record-breaking experimental demonstrations on large-capacity/long-distance wireless mm-wave signal delivery based on photonic mm-wave generation techniques as well as the favorable coordination of multiple multi-dimensional multiplexing techniques introduced in Fig. 29 [72]. For the large-capacity wireless mm-wave signal delivery, they first experimentally demonstrated up to 108-Gb/s polarization-division multiplexed quaternary phase shift keying (PDM-QPSK) wireless mm-wave signal delivery at W-band [73], up to 400-Gb/s hybrid PDM-QPSK and polarization-division-multiplexing 16-ary quadrature amplitude modulation (PDM-16QAM) wireless mm-wave signal delivery at both Q-band and W-band [74], and up to 432-Gb/s PDM-16QAM wireless mm-wave signal delivery at W-band [75]. For both large-capacity and long-distance wireless mm-wave signal delivery, they successfully achieved field trial demonstrations of 20-Gb/s PDM-QPSK signal delivery over 1.7-km wireless distance at W-band [76], 80-Gb/s PDM-QPSK signal delivery over 300-m wireless distance at W-band [77], and 100-Gb/s QPSK signal delivery over 100-m wireless distance at W-band [78].

To characterize the spectral responses of optical devices with ultra-high resolution [79], optical vector analyzers (OVAs) based on optical single-sideband (OSSB) modulation were developed by Prof. Pan from Nanjing University of Aeronautics and Astronautics (NUAA) [80], which

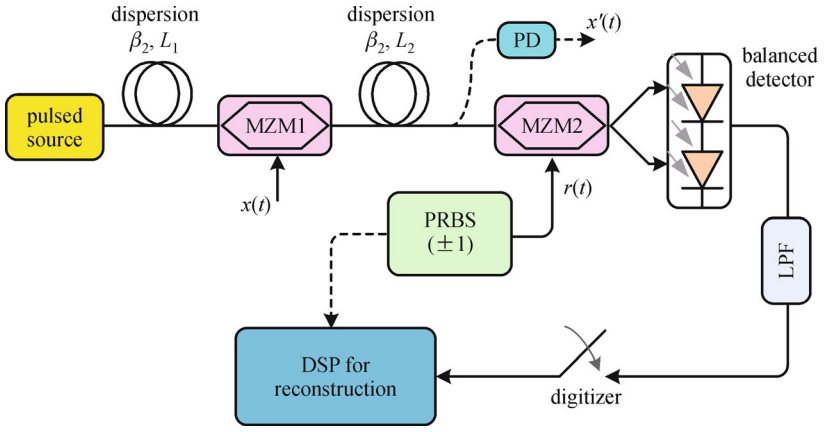

Fig. 25 Schematic illustration of the sub-Nyquist sampled photonic analog-to-digital converter based on of the techniques of photonic time stretch and compressive sensing.LPF: low pass filter; DSP: digital signal processing; PRBS: pseudorandom binary sequence [55–61]

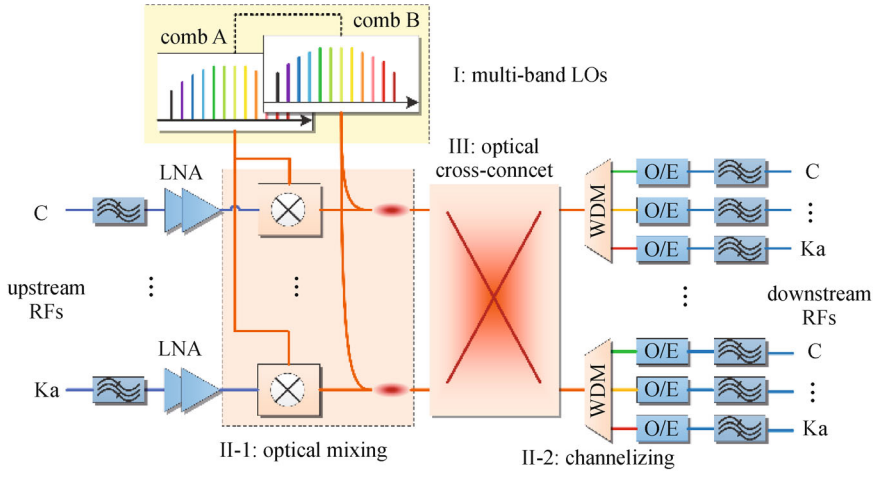

Fig. 26 Conceptual architecture of multi-band satellite repeater based on optical frequency combs. LNA: low noise amplifier; WDM: wavelength-division multiplexing [62,63]

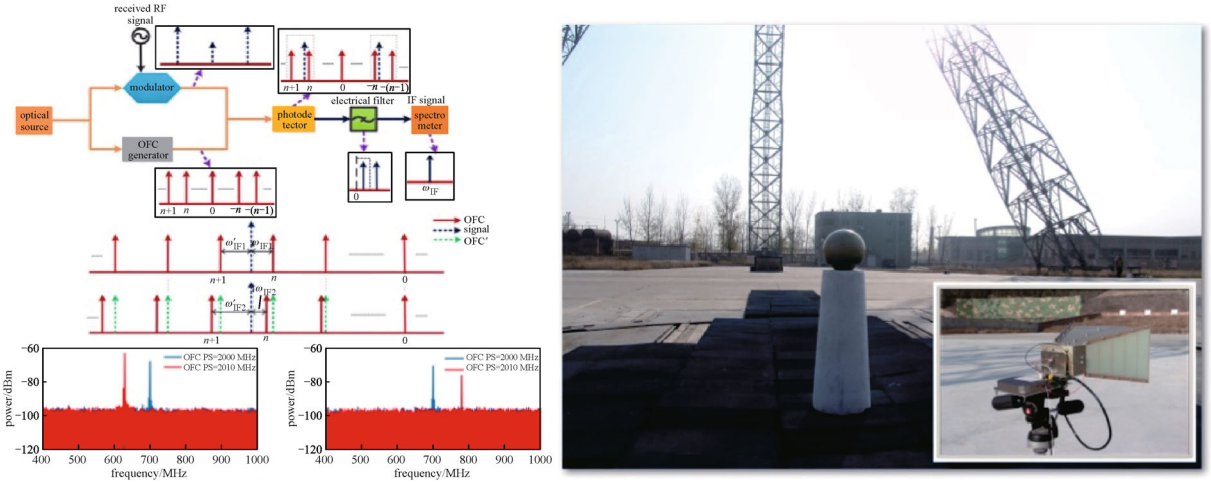

Fig. 27 MWP research activities in Beihang University based on OFCs [64]

sweep the frequency and analyze the responses using the mature and high-resolution microwave technologies. Figure 30 shows the schematic diagram of the OSSB-based OVA. Although the reported resolution has been better than 0.8 fm [80], its application is restricted by the limited measurement range and measurement errors due to the O/E and E/O conversions.

In their recent work, the measurement range of the OSSB-OVA was boosted based on an OFC. With each carrier in the OFC to achieve the magnitude and phase responses in a certain range, the measurement range of the OSSB-based OVA is extended by about n times if an n-comb-line OFC is applied. In the experiment, a 105-GHz measurement range is achieved by employing a 5-comb-line OFC with 20-GHz frequency spacing. In the OSSB-based OVA, the frequency responses are only carried by the beat note of the optical carrier and one of the first-order sideband. By suppressing the optical carrier, the desired beat note is removed, leaving only the measurement errors. By simultaneously detecting the OSSB with and without carrier adopting balanced PD, the accurate frequency responses can be obtained with a large dynamic range. Thus, an OSSB-based OVA with wide measurement range, ultrahigh-resolution, and high accuracy can be achieved.

A conceptual software-defined satellite payload based on MWP has been proposed and investigated by Prof. Pan from NUAA [81], as shown in Fig. 2 [31]. By introducing microwave photonic components and subsystems to realize multiple LO generation and distribution, frequency conversion, analog-to-digital conversion (ADC), digital to analog conversion (DAC), switching, and multi-beam-forming functions, the proposed satellite payload can implement high-efficiency on-board parallel signal processing with enhanced capacity and significantly reduced mass, volume, and power consumption.

In their recent work, the potential to apply the photonic technologies to the satellite payloads is studied. Technologies such as the optical LO sources generation based on OEO, parallel photonic microwave FMIX for signal transportation and photonic signal switching based on high speed optical switch have been demonstrated. A 2×2 photonic satellite repeater experimental demonstration for switching of HD video signals with 1.5-Gb/s data rate is shown in Fig. 31. Two HD video signals are up-converted to the Ku-band (16 GHz) and transmitted to the free space through two antennas. In the receive site of the microwave photonic repeater, the received signals from the two antennas are modulated onto two different optical carriers. The two optical signals are simultaneously down-converted to the IF-band by multiply with an OEO-based LO signal, thanks to the parallel FMIX by a photonic mixer. The downconverted IF signals are then separated by a wavelength-division de-multiplexer. A high-speed optical micro-electro-mechanical system (MEMS) switch controlled by computer is used for the switching of the two channels. After photodetection and further downconversion, the switched HD video signals are sent to separate displayers. The HD video signals are successfully transmitted to the receiver site through the photonic-based payload, and the HD signal can be flexibly exchanged in the analog domain by the optical MEMS switch without cross interference.

Construction of distributed radar systems based on microwave photonic technologies has been researched [82]. A distributed multiple-input multiple-output chaotic radar using wavelength-division multiplexing (WDM) technology is proposed and demonstrated [82], as shown in Fig. 32. The wideband quasi-orthogonal chaotic signals are generated by different OEOs, and emitted by separated antennas to gain spatial diversity against the fluctuation of a target's radar cross section. In this way, the detection capability will be enhanced. The signals received by the receive antennas and the reference signals from the OEOs are delivered to the central station for joint processing by exploiting WDM technology. The centralized signal processing avoids precise time synchronization of the distributed system and greatly simplifies the remote units, which improves the localization accuracy of the entire system. A proof of concept experiment for two-dimensional localization of a metal target is demonstrated, with a maximum position error of less than 6.5 cm.

Compared to many other techniques for photonic UWB

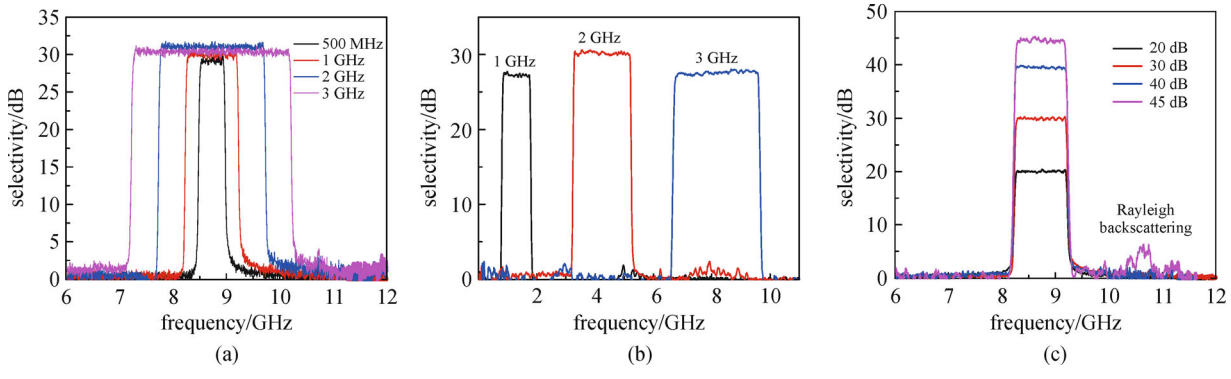

Fig. 28 Filter bandwidth, central frequency and selectivity tuning of SBS based MPF [67–71]

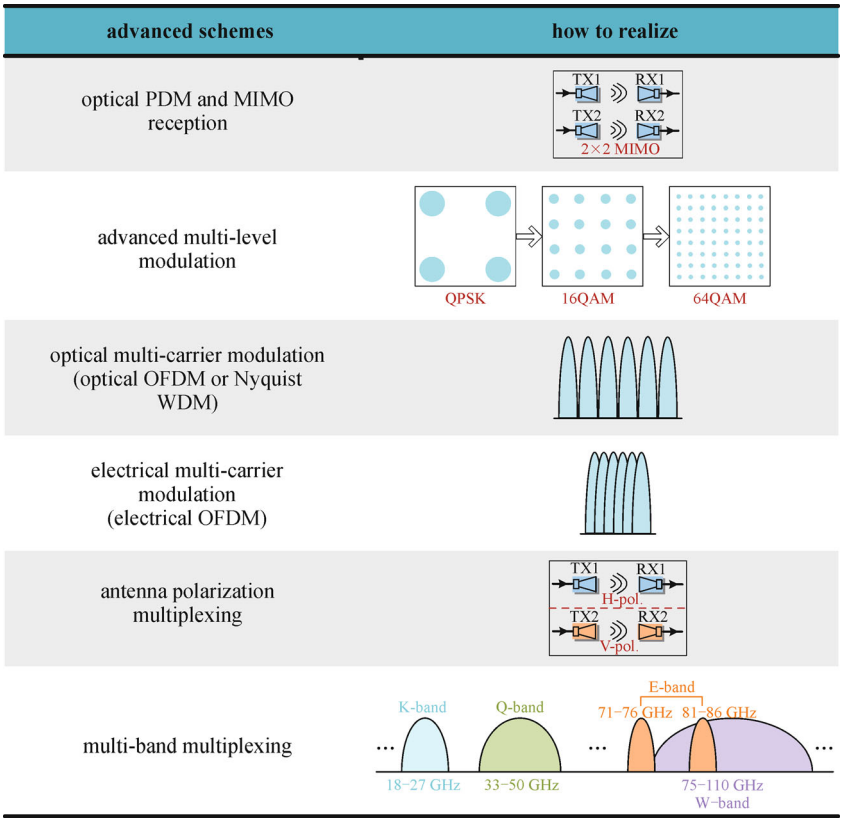

Fig. 29 Different approaches for the realization of large-capacity/long-distance wireless mm-wave signal transmission [72]. MIMO: multiple-input multiple-output

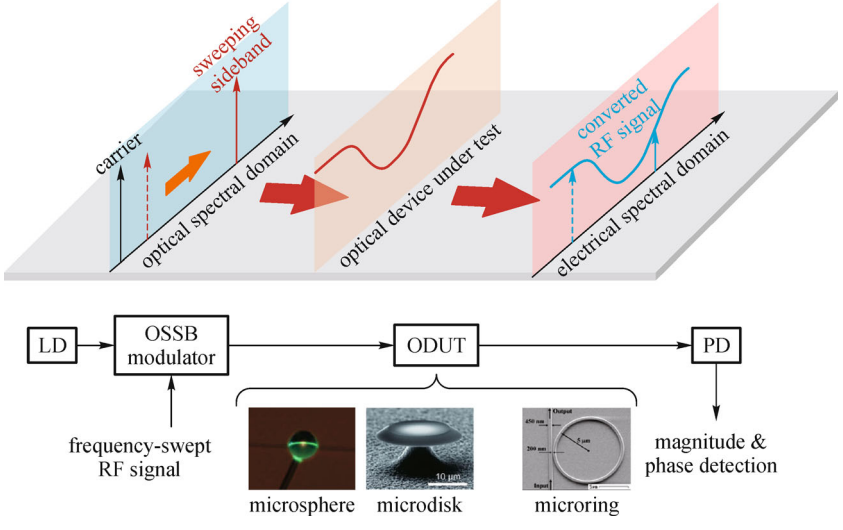

Fig. 30 Schematic diagram of the high-resolution optical vector analyzer based on optical single-sideband modulation [80]. OSSB: optical single-sideband; ODUT: optical device-under-test

signal generation based on impulse radio, Wang et al. proposed novel methods to generate noise-like UWB signal in optical domain, which was called chaotic UWB signal [83,84]. Based on the chaotic dynamics of an optically injected semiconductor laser with optical feedback, the chaotic UWB signal with a fractional bandwidth of 116% and the central frequency of 6.88 GHz was experimentally generated [84]. The experimental setup was shown in Fig. 33, and the generated chaotic UWB signal was shown in Fig. 34. The spectrum of the generated

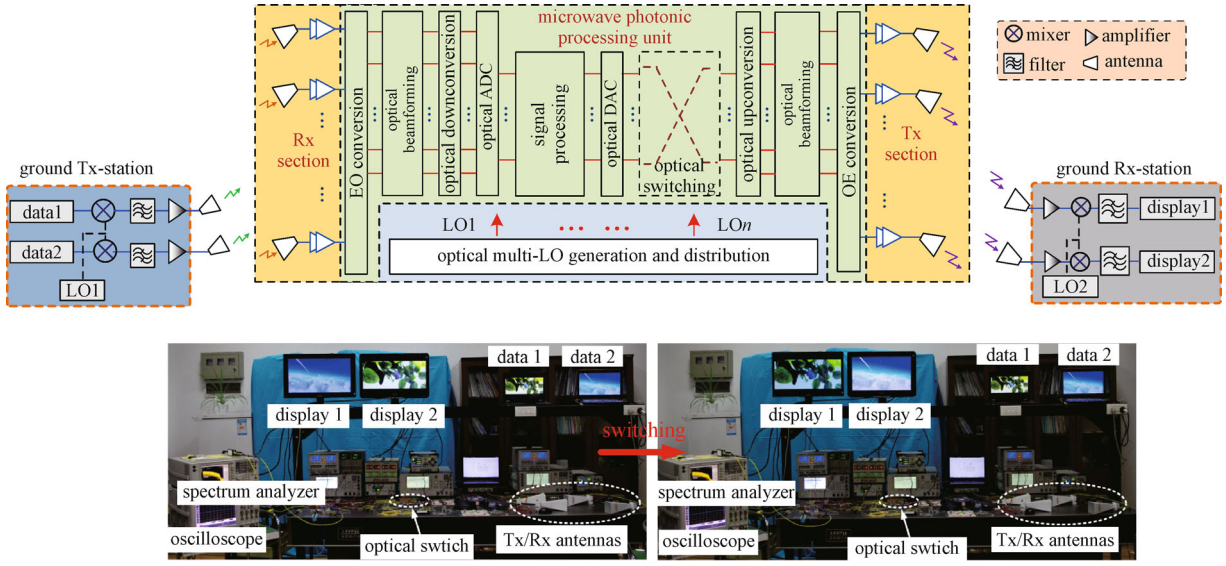

Fig. 31 Block diagram scheme of a conceptual software-defined satellite payload based on MWP; experimental demonstration of 2 ×2 microwave photonic switch for HD video [81]

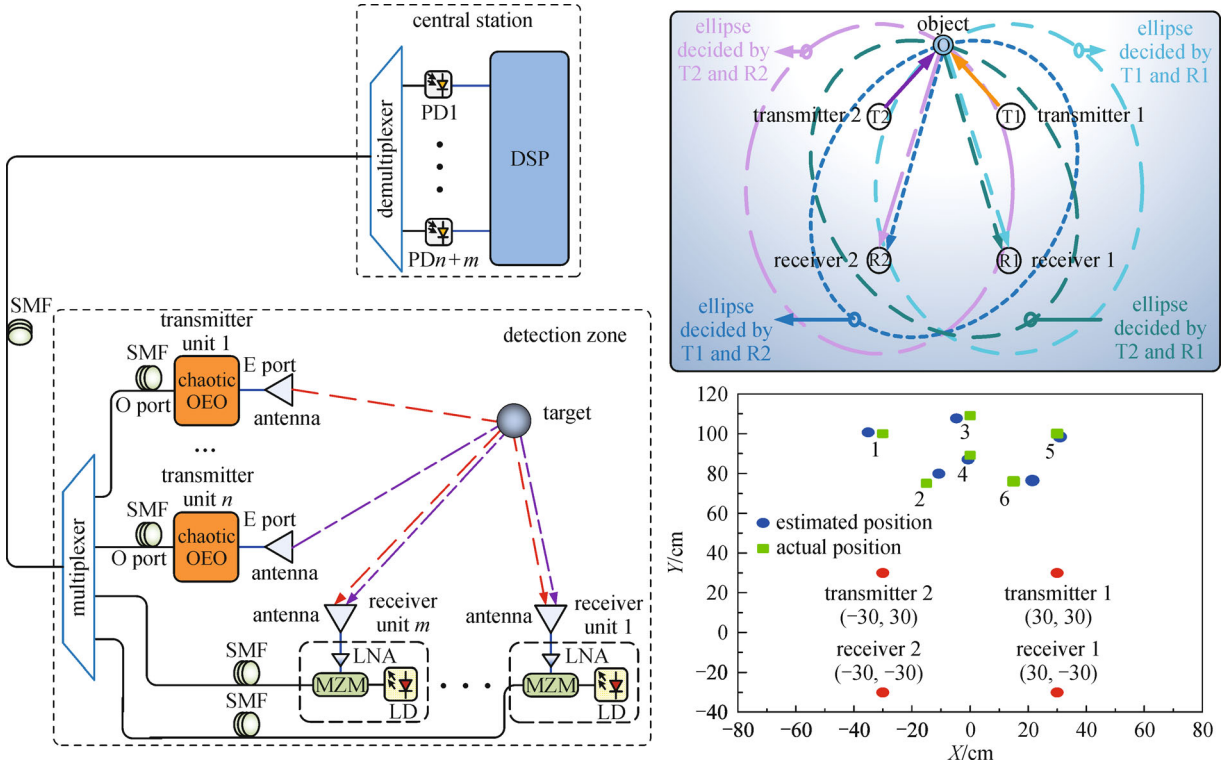

Fig. 32 Schematic diagram of the proposed distributed MIMO chaotic radar based on WDM technology, geometric model of two-dimensional localization with two transmitters and two receivers, and the geometric locations of six samples of the estimated positions and their corresponding actual positions [82]

chaotic UWB signal was in full compliance with the Federal Communications Commission (FCC) spectral mask. Moreover, by controlling the injection strength and frequency detuning of the chaotic laser, the generated UWB signals' spectrum bandwidth and central frequency could be flexibly adjusted in a certain range. Furthermore, based on the photonic chaotic UWB signal, they proposed a UWB radar system for remote ranging [85] and a

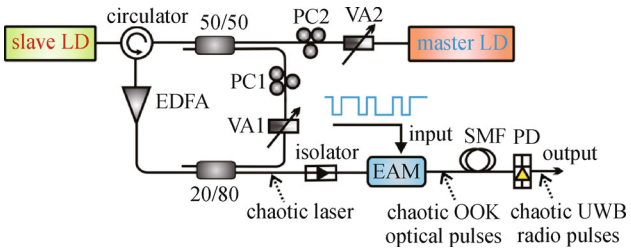

Fig. 33 Experimental setup for photonic chaotic UWB signal generation [83]. VA: variable attenuator; EAM: electro-absorption modulator; OOK: on-off keying

microwave-photonic sensor for remote water-level monitoring [86]. This remote radar system not only realizes the remote control of the radar, but also has a high range resolution with antijamming ability, which can be used for the military radar in hilltops under bad conditions and the radar systems of islands, dangerous areas, and harsh industrial environments. The microwave-photonic sensor has advantages in remote real-time water-level measurements and high range resolution, which can provide early warning of events for flood control projects, coal mines production, the flood control stations of alpine valleys.

Radio over fiber technology has great potential applications in many fields, especially for the high frequency microwave signal transmission over a long fiber distance. However, the dispersion induced RF power fading is the main factor deteriorating the performance of radio over fiber system with the conventional DSB. The tunable optical filter based on the integrated waveguide microring resonator was designed and fabricated with the UV-soft selective imprint technique, which has the tunable notch depth and the tunable central frequency. As shown in Fig. 35, it was utilized to filter out one sideband of the DSB signal. The chromatic dispersion induced RF power fading was overcome effectively by the tunable ring resonator with the demonstration of the successful transmission of 7.2 GHz microwave signal over 70 km single-mode fiber (SMF) [87].

Prof. Li from IOS-CAS proposed a simple method to realize stable radio-frequency phase distribution over optical fiber by phase-drift auto-cancellation without using any assistant LO source, as shown in Fig. 36 [88]. Besides, neither active phase discrimination nor dynamic phase tracking/compensation is required in this open-loop

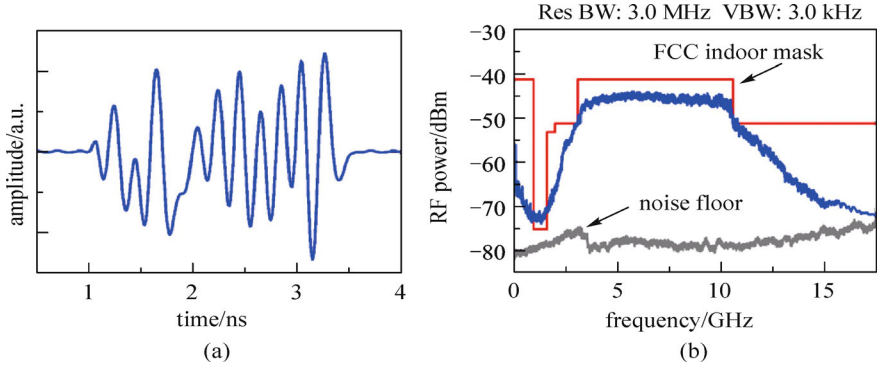

Fig. 34 Waveforms (a) and RF spectra (b) of the experimentally generated chaotic UWB signal

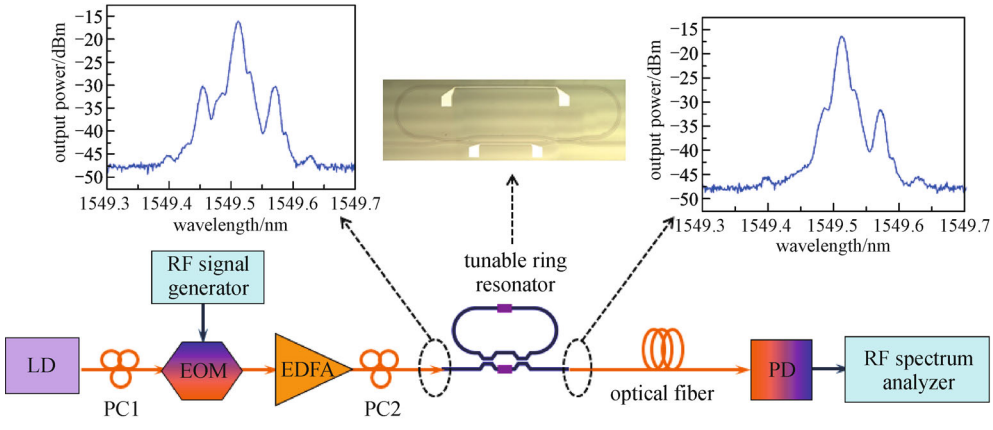

Fig. 35 Single sideband (SSB) radio over fiber by using the integrated waveguide tunable microring resonator [87]

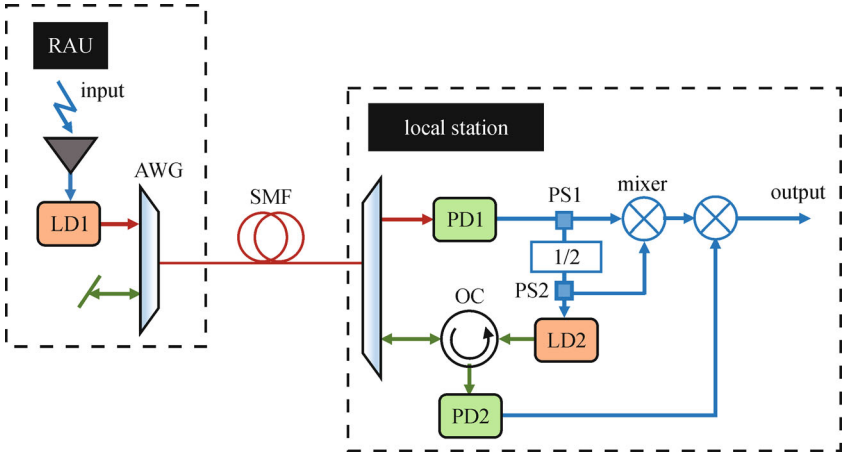

Fig. 36 Schematic diagram of the stable RF phase distribution scheme [88]. AWG: array waveguide grating; PS: power splitter; OC: optical circulator

design. The phase-drifts of the RF signal induced by fiber-length variations are eliminated automatically via RF mixing. Since no assistant LO signal is involved in our scheme, the complicated frequency-estimation of the received RF signal as well as the dynamic frequency-locking between the LO and the received RF signal is not required anymore, which greatly simplifies the system. Experimentally, phase-drift-free RF signal is successfully achieved. The root-mean-square (RMS) timing jitter is 0.76 ps when a tunable optical delay line (TODL) inserted between the remote antenna unit (RAU) and local station is changed from 0 to 300 ps.

To characterize a device-under-test (DUT) with ultra-fine transmission response, optical vector network analyzer (OVNA) is a promising device. The OVNA based on single-sideband modulation usually suffers from huge measurement errors due to the nonlinearity of the modulator. Prof. Li proposed an OVNA with improved accuracy based on dual-parallel Mach-Zehnder modulator (DPMZM). By properly setting the bias voltage of the DPMZM, the measurement error is significantly reduced, as shown in Fig. 37 [89].

IFM based on photonic techniques has attracted great attention recently. An IFM system is usually used in radars and electronic warfare systems for detecting and classifying unknown signals. Prof. Li proposed an IFM system with adjustable measurement range and resolution based on SBS in optical fiber, see Fig. 38 [90]. The proposed technique can be switchable between a wideband tunable narrow measurement range (~2 GHz) with high resolution (±0.05 GHz) and a fixed wide measurement range (12 GHz) with moderate resolution (±0.25 GHz).

The implementation of all-optical circuits for computing, information processing, generation and networking could overcome the severe speed limitations currently imposed by electronic-based systems [91–123]. A

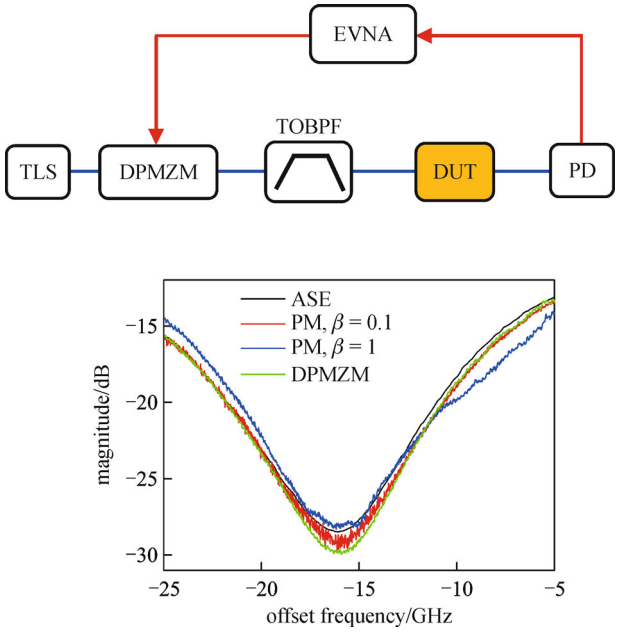

Fig. 37 Proposed OVNA with improved accuracy [89]. TLS: tunable laser source; TOBPF: tunable optical bandpass filter; EVNA: electrical vector network analyzer; ASE: amplified spontaneous emission

promising approach toward the implementation of ultrafast all-optical circuits is to emulate the developments in the electronic domain, i.e., to follow similar component and design strategies, using photonic technologies [91–94]. For this purpose, high-speed optical signal processors, such as optical differentiator [95–101], integrator [102–105], Fourier transformer [106,107] and Hilbert transformer [108,109], have recently attracted an increasing interest in optical communications, pulse shaping or sensing applications that use optical signals [110–114].

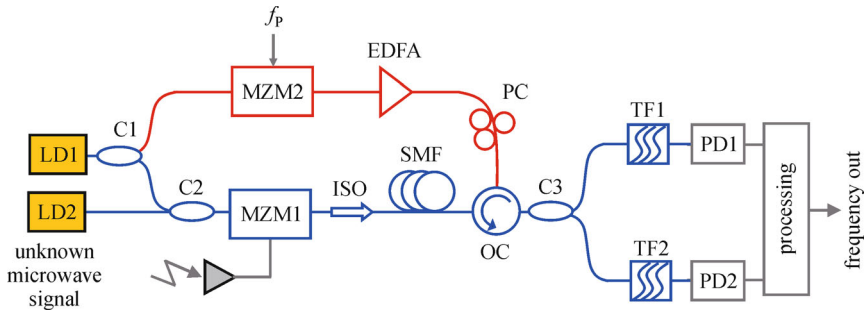

Fig. 38 Proposed IFM system.ISO: isolator [90]

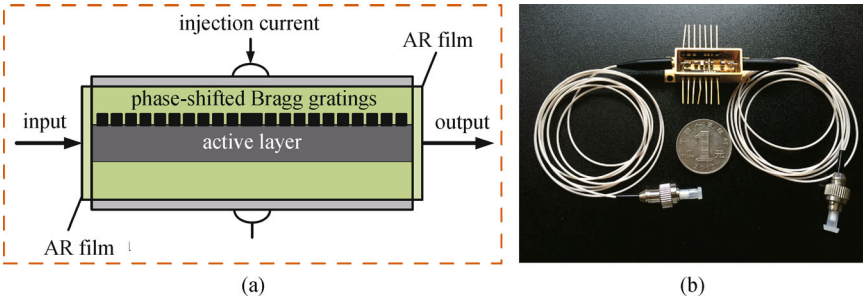

Fig. 39 Phase-shifted DFB-SOA. (a) Schematic diagram and (b) the physical image of the packaged phase-shifted DFB-SOA [125]

Prof. Li from IOS-CAS has focused his research topics on all-optical signal processor [124,125]. Recently, he proposed and experimentally demonstrated an analog optical signal processor based on a phase-shifted DFB-SOA and an optical filter [125]. The proposed analog optical signal processor can be reconfigured to perform signal processing functions including ordinary differential equation solving and temporal intensity differentiation. The reconfigurability is achieved by controlling the injection currents. Our demonstration provides a simple and effective solution for all-optical signal processing and computing.

4 Conclusion

Recent progresses of MWP have been reviewed including the main projects and representative results from almost all the active research teams in China. In the past five years, many impressive progresses in MWP devices and subsystem have been made to support the development of national major assignments. Compare to the rapid development of MWP subsystem, the IMWP devices should be further largely improved in the near future. In the next five years, the national major research and development program has considered MWP, in particular IMWP devices, as one of the key enabling technologies for improving the performance of information system.

Acknowledgements We would like to thank all the colleagues who have been involved into these reported works in China and collaborated internationally. We would like to thank the supporting of the National High-Tech Research & Development Program of China (Nos. 2011AA010303, 2013AA014201 and 2011AA010305) and the National Natural Science Foundation of China (Grant Nos. 61177080, 61377002, 61321063 and 61090391). Ming Li was supported in part by the "Thousand Young Talent" program.

References

1. Capmany J, Novak D. Microwave photonics combines two worlds. Nature Photonics, 2007, 1(6): 319–330
2. Yao J. Microwave photonics. Journal of Lightwave Technology, 2009, 27(3): 314–335
3. Waterhouse R, Novack D. Realizing 5G: microwave photonics for 5G mobile wireless systems. IEEE Microwave Magazine, 2015, 16 (8): 84–92
4. Iezekiel S, Burla M, Klamkin J, Marpaung D, Capmany J. RF engineering meets optoelectronics: progress in integrated microwave photonics. IEEE Microwave Magazine, 2015, 16(8): 28–45
5. Ghelfi P, Laghezza F, Scotti F, Serafino G, Pinna S, Onori D, Lazzeri E, Bogoni A. Photonics in radar systems: RF integration for state-of-the-art functionality. IEEE Microwave Magazine, 2015, 16(8): 74–83
6. Capmany J, Li G, Lim C, Yao J. Microwave photonics: current challenges towards widespread application. Optics Express, 2013, 21(19): 22862–22867
7. Marpaung D, Roeloffzen C, Heideman R, Leinse A, Sales S, Capmany J. Integrated microwave photonics. Laser & Photonics Reviews, 2013, 7(4): 506–538

8. Xie L, Man J W, Wang B J, Liu Y, Wang X, Yuan H Q, Zhao L J, Zhu H L, Zhu N H, Wang W. 24-GHz directly modulated DFB laser modules for analog applications. IEEE Photonics Technology Letters, 2012, 24(5): 407–409
9. Li S, Zheng X, Zhang H, Zhou B. Compensation of dispersion-induced power fading for highly linear radio-over-fiber link using carrier phase-shifted double sideband modulation. Optics Letters, 2011, 36(4): 546–548
10. Zheng X, Zhang G, Li S, Zhang H, Zhou B. All-optical signal processing for linearity enhancement of Mach-Zehnder modulators. Chinese Science Bulletin, 2014, 59(22): 2655–2660
11. Wang X, Liu Z, Wang S, Sun D, Dong Y, Hu W. Photonic radio-frequency dissemination via optical fiber with high-phase stability. Optics Letters, 2015, 40(11): 2618–2621
12. Deng Y, Li M, Tang J, Sun S, Huang N, Zhu N. Widely tunable single-passband microwave photonic filter based on DFB-SOA-assisted optical carrier recovery. IEEE Photonics Journal, 2015, 7 (5): 5501108-1–5501108-8
13. Zhu N H, Zhang H G, Man J W, Zhu H L, Ke J H, Liu Y, Wang X, Yuan H Q, Xie L, Wang W. Microwave generation in an electro-absorption modulator integrated with a DFB laser subject to optical injection. Optics Express, 2009, 17(24): 22114–22123
14. Pan B, Lu D, Sun Y, Yu L, Zhang L, Zhao L. Tunable optical microwave generation using self-injection locked monolithic dual-wavelength amplified feedback laser. Optics Letters, 2014, 39(22): 6395–6398
15. Lu D, Pan B, Chen H, Zhao L. Frequency-tunable optoelectronic oscillator using a dual-mode amplified feedback laser as an electrically controlled active microwave photonic filter. Optics Letters, 2015, 40(18): 4340–4343
16. Zou L, Huang Y, Lv X, Liu B, Long H, Yang Y, Xiao J, Du Y. Modulation characteristics and microwave generation for AlGaInAs/InP microring lasers under four-wave mixing. Photonics Research, 2014, 2(6): 177–181
17. Zou L, Liu B, Lv X, Yang Y, Xiao J, Huang Y. Integrated semiconductor twin-microdisk laser under mutually optical injection. Applied Physics Letters, 2015, 106(19): 191107-1–191107-4
18. Yu H, Chen M, Guo Q, Hoekman M, Chen H, Leinse A, Heideman R G, Yang S, Xie S. A full-band RF photonic receiver based on the integrated ultra-high Q bandpass filter. In: Proceedings of Optical Fiber Communication Conference and Exhibition. 2015, 1–3
19. Yu H, Chen M, Guo Q, Hoekman M, Chen H, Leinse A, Heideman R G, Mateman R, Yang S, Xie S. All-optical full-band RF receiver based on an integrated ultra-high-*Q* bandpass filter. Journal of Lightwave Technology, 2016, 34(2): 701–706
20. Shi T, Xiong B, Sun C, Luo Y. Back-to-back UTC-PDs with high responsivity, high saturation current and wide bandwidth. IEEE Photonics Technology Letters, 2013, 25(2): 136–139
21. Huang J, Sun C, Song Y, Xiong B, Luo Y. Influence of master laser's lineshape on the optically generated microwave carrier by injection locking. Applied Physics Express, 2009, 2(7): 072502-1–072502-3
22. Long Y, Wang J. Ultra-high peak rejection notch microwave photonic filter using a single silicon microring resonator. Optics Express, 2015, 23(14): 17739–17750
23. Dong J, Liu L, Gao D, Yu Y, Zheng A, Yang T, Zhang X. Compact notch microwave photonic filters using on-chip integrated microring resonators. IEEE Photonics Journal, 2013, 5(2): 5500307-1–5500307-8
24. Xie J, Zhou L, Li Z, Wang J, Chen J. Seven-bit reconfigurable optical true time delay line based on silicon integration. Optics Express, 2014, 22(19): 22707–22715
25. Wu J, Peng J, Liu B, Pan T, Zhou H, Mao J, Yang Y, Qiu C, Su Y. Passive silicon photonic devices for microwave photonic signal processing. Optics Communications, 2015, doi:10.1016/j.optcom.2015.07.045
26. Wu X M, Man J W, Xie L, Liu Y, Qi X Q, Wang L X, Liu J G, Zhu N H. Novel method for frequency response measurement of optoelectronic devices. IEEE Photonics Technology Letters, 2012, 24(7): 575–577
27. Zhang S, Wang H, Zou X, Zhang Y, Lu R, Liu Y. Extinction-ratio-independent electrical method for measuring chirp parameters of Mach-Zehnder modulators using frequency-shifted heterodyne. Optics Letters, 2015, 40(12): 2854–2857
28. Wang H, Zhang S, Zou X, Zhang Y, Lu R, Zhang Z, Liu Y. Calibration-free and bias-drift-free microwave characterization of dual-drive Mach-Zehnder modulators using heterodyne mixing. Optical Engineering, 2016, 55(3): 031109-1–031109-6
29. Zhang S, Wang H, Zou X, Zhang Y, Lu R, Liu Y. Self-calibrating measurement of high-speed electro-optic phase modulators based on two-tone modulation. Optics Letters, 2014, 39(12): 3504–3507
30. Zhang S, Wang H, Zou X, Zhang Y, Lu R, Liu Y. Calibration-free electrical spectrum analysis for microwave characterization of optical phase modulators using frequency-shifted heterodyning. IEEE Photonics Journal, 2014, 6(4): 5501008-1–5501008-8
31. Zhang S, Wang H, Zou X, Zhang Y, Lu R, Li H, Liu Y. Optical frequency-detuned heterodyne for self-referenced measurement of photodetectors. IEEE Photonics Technology Letters, 2015, 27(9): 1014–1017
32. Li S, Zheng X, Zhang H, Zhou B. Compensation of dispersion-induced power fading for highly linear radio-over-fiber link using carrier phase-shifted double sideband modulation. Optics Letters, 2011, 36(4): 546–548
33. Zheng X, Zhang G, Li S, Zhang H, Zhou B. All-optical signal processing for linearity enhancement of Mach-Zehnder modulators. Chinese Science Bulletin, 2014, 59(22): 2655–2660
34. Zhang G, Zheng X, Li S, Zhang H, Zhou B. Postcompensation for nonlinearity of Mach-Zehnder modulator in radio-over-fiber system based on second-order optical sideband processing. Optics Letters, 2012, 37(5): 806–808
35. Zhang G, Li S, Zheng X, Zhang H, Zhou B, Xiang P. Dynamic range improvement strategy for Mach-Zehnder modulators in microwave/millimeter-wave ROF links. Optics Express, 2012, 20 (15): 17214–17219
36. Zhang G, Zheng X, Li S.Millimeter-wave over fiber transmitter with subcarrier upconversion and nonlinear compensation. In: Proceedings of Asia-Pacific Microwave Photonics Conference, 2012
37. Song Y, Li S, Zheng X, Zhang H, Zhou B. True time-delay line with high resolution and wide range employing dispersion and optical spectrum processing. Optics Letters, 2013, 38(17): 3245–3248

38. Li L, Zhang G, Zheng X, Li S, Zhang H, Zhou B. Suppression for dispersion induced phase noise of an optically generated millimeter wave employing optical spectrum processing. Optics Letters, 2012, 37(19): 3987–3989
39. Zhou X, Zheng X, Wen H, Zhang H, Zhou B. Optical arbitrary waveform generator applicable to pulse generation and chromatic dispersion compensation of a remote UWB over fiber system. Optics Express, 2011, 19(26): B391–B398
40. Xue X, Zheng X, Zhang H, Zhou B. Widely tunable single-bandpass microwave photonic filter employing a non-sliced broadband optical source. Optics Express, 2011, 19(19): 18423–18429
41. Xue X, Zheng X, Zhang H, Zhou B. Highly reconfigurable microwave photonic single-bandpass filter with complex continuous-time impulse responses. Optics Express, 2012, 20(24): 26929–26934
42. Yang J, Chan E H W, Wang X, Feng X, Guan B. Broadband photonic microwave phase shifter based on controlling two RF modulation sidebands via a Fourier-domain optical processor. Optics Express, 2015, 23(9): 12100–12110
43. Liu J, Guo N, Li Z, Yu C, Lu C. Ultrahigh-*Q* microwave photonic filter with tunable *Q* value utilizing cascaded optical-electrical feedback loops. Optics Letters, 2013, 38(21): 4304–4307
44. Xin X, Zhang L, Liu B, Yu J. Dynamic λ-OFDMA with selective multicast overlaid. Optics Express, 2011, 19(8): 7847–7855
45. Zhang L, Xin X, Liu B, Zhao K, Yu C. A novel WDM-OFDM-PON architecture with centralized lightwave and PolSK-assisted multicast overlay. In: Proceedings of National Fiber Optic Engineers Conference, Optical Society of America. 2010, JThA25
46. Liu B, Xin X, Zhang L, Yu J. 109.92-Gb/s WDM-OFDMA uni-PON with dynamic resource allocation and variable rate access. Optics Express, 2012, 20(10): 10552–10561
47. Zhang L, Xin X, Liu B, Wang Y, Yu J, Yu C. OFDM modulated WDM-ROF system based on PCF-supercontinuum. Optics Express, 2010, 18(14): 15003–15008
48. Wang X, Liu Z, Wang S, Sun D, Dong Y, Hu W. Photonic radio-frequency dissemination via optical fiber with high-phase stability. Optics Letters, 2015, 40(11): 2618–2621
49. Sun D, Dong Y, Shi H, Xia Z, Liu Z, Wang S, Xie W, Hu W. Distribution of high-stability 100.04 GHz millimeter wave signal over 60 km optical fiber with fast phase-error-correcting capability. Optics Letters, 2014, 39(10): 2849–2852
50. Sun D, Dong Y, Yi L, Wang S, Shi H, Xia Z, Xie W, Hu W. Photonic generation of millimeter and terahertz waves with high phase stability. Optics Letters, 2014, 39(6): 1493–1496
51. Wang S, Sun D, Dong Y, Xie W, Shi H, Yi L, Hu W. Distribution of high-stability 10 GHz local oscillator over 100 km optical fiber with accurate phase-correction system. Optics Letters, 2014, 39(4): 888–891
52. Feng D, Xie H, Chen G, Qian L, Sun J. Simultaneous generation of a frequency-multiplied and phase-shifted microwave signal with large tunability. Optics Express, 2014, 22(15): 18372–18378
53. Feng D, Sun J, Xie H. Control of the optical carrier to sideband ratio in optical double/single sideband modulation by the phase variation of RF signals. Optics Communications, 2015, 353: 30–34
54. Feng D, Xie H, Qian L, Bai Q, Sun J. Photonic approach for microwave frequency measurement with adjustable measurement range and resolution using birefringence effect in highly non-linear fiber. Optics Express, 2015, 23(13): 17613–17621
55. Chi H, Mei Y, Chen Y, Wang D, Zheng S, Jin X, Zhang X. Microwave spectral analysis based on photonic compressive sampling with random demodulation. Optics Letters, 2012, 37 (22): 4636–4638
56. Chen Y, Yu X, Chi H, Jin X, Zhang X, Zheng S, Galili M. Compressive sensing in a photonic link with optical integration. Optics Letters, 2014, 39(8): 2222–2224
57. Chen Y, Yu X, Chi H, Zheng S, Zhang X, Jin X, Galili M. Compressive sensing with a microwave photonic filter. Optics Communications, 2015, 338: 428–432
58. Zhu Z, Chi H, Zheng S, Jin T, Jin X, Zhang X. Analysis of compressive sensing with optical mixing using a spatial light modulator. Applied Optics, 2015, 54(8): 1894–1899
59. Chen Y, Ding Y, Zhu Z, Chi H, Zheng S, Zhang X, Jin X, Galili M, Yu X. Photonic compressive sensing with a micro-ring-resonator-based microwave photonic filter. Optics Communications, 2015, doi: 10.1016/j.optcom.2015.06.080
60. Chi H, Chen Y, Mei Y, Jin X, Zheng S, Zhang X. Microwave spectrum sensing based on photonic time stretch and compressive sampling. Optics Letters, 2013, 38(2): 136–138
61. Chen Y, Chi H, Jin T, Zheng S, Jin X, Zhang X. Sub-Nyquist sampled analog-to-digital conversion based on photonic time stretch and compressive sensing with optical random mixing. Journal of Lightwave Technology, 2013, 31(21): 3395–3401
62. Yang X, Xu K, Yin J, Dai Y, Yin F, Li J, Lu H, Liu T, Ji Y. Optical frequency comb based multi-band microwave frequency conversion for satellite applications. Optics Express, 2014, 22(1): 869–877
63. Xu K, Wang R, Dai Y, Yin F, Li J, Ji Y, Lin J. Microwave photonics: radio-over-fiber links, systems, and applications. Photonics Research, 2014, 2(4): B54–B63
64. Yan J, Xia Z, Zhang S, Bai M, Zheng Z. A flexible waveforms generator based on a single dual-parallel Mach-Zehnder modulator. Optics Communications, 2015, 334: 31–34
65. Fang X, Bai M, Ye X, Miao J, Zheng Z. Ultra-broadband microwave frequency down-conversion based on optical frequency comb. Optics Express, 2015, 23(13): 17111–17119
66. Zhao X, Zheng Z, Liu L, Wang Q, Chen H, Liu J. Fast, long-scan-range pump-probe measurement based on asynchronous sampling using a dual-wavelength mode-locked fiber laser. Optics Express, 2012, 20(23): 25584–25589
67. Wei W, Yi L, Jaouën Y, Hu W. Bandwidth-tunable narrowband rectangular optical filter based on stimulated Brillouin scattering in optical fiber. Optics Express, 2014, 22(19): 23249–23260
68. Wei W, Yi L, Jaouën Y, Morvan M, Hu W. Brillouin rectangular optical filter with improved selectivity and noise performance. IEEE Photonics Technology Letters, 2015, 27(15): 1593–1596
69. Yi L, Wei W, Jaouen Y, Hu W. Ideal rectangular microwave photonic filter with high selectivity based on stimulated Brillouin scattering. In: Proceedings of Optical Fiber Communication Conference, Optical Society of America. 2015, Tu3F.5
70. Yi L, Wei W, Jaouen Y, Shi M, Han B, Morvan M, Hu W. Polarization-independent rectangular microwave photonic filter

based on stimulated brillouin scattering. Journal of Lightwave Technology, 2016, 34(2): 669–675
71. Yi L, Wei W, Hu W. Design and performance evaluation of narrowband rectangula optical filter based on stimulated Brillouin scattering in fiber. In: Proceedings of International Conference on Optical Communications and Networks. 2014, 1–2
72. Yu J, Li X, Chi N. Faster than fiber: over 100-Gb/s signal delivery in fiber wireless integration system. Optics Express, 2013, 21(19): 22885–22904
73. Li X, Dong Z, Yu J, Chi N, Shao Y, Chang G K. Fiber-wireless transmission system of 108 Gb/s data over 80 km fiber and 2×2 multiple-input multiple-output wireless links at 100 GHz W-band frequency. Optics Letters, 2012, 37(24): 5106–5108
74. Li X, Yu J, Zhang J, Dong Z, Li F, Chi N. A 400G optical wireless integration delivery system. Optics Express, 2013, 21(16): 18812–18819
75. Yu J, Li X, Zhang J, Xiao J. 432-Gb/s PDM-16QAM signal wireless delivery at W-band using optical and antenna polarization multiplexing. In: Proceedings of European Conference on Optical Communication. 2014, 1–3
76. Xiao J, Yu J, Li X, Xu Y, Zhang Z, Chen L. 40-Gb/s PDM-QPSK signal transmission over 160-m wireless distance at W-band. Optics Letters, 2015, 40(6): 998–1001
77. Li X, Yu J, Zhang Z, Xu Y. Field trial of 80-Gb/s PDM-QPSK signal delivery over 300-m wireless distance with MIMO and antenna polarization multiplexing at W-band. In: Proceedings of Optical Fiber Communication Conference, Optical Society of America. 2015, Th5A.5
78. Li X, Yu J, Xiao J. 100^3 (100 Gb/s×100 m×100 GHz) optical wireless system. In: Proceedings of European Conference on Optical Communication. 2015, 1–3
79. Román J E, Frankel M Y, Esman R D. Spectral characterization of fiber gratings with high resolution. Optics Letters, 1998, 23(12): 939–941
80. Tang Z, Pan S, Yao J. A high resolution optical vector network analyzer based on a wideband and wavelength-tunable optical single-sideband modulator. Optics Express, 2012, 20(6): 6555–6560
81. Pan S, Zhu D, Liu S, Xu K, Dai Y, Wang T, Liu J, Zhu N, Xue Y, Liu N. Satellite payloads pay off. IEEE Microwave Magazine, 2015, 16(8): 61–73
82. Fu J, Chen X, Pan S. A fiber-distributed multistatic ultra-wideband radar. In: Proceedings of International Conference on Optical Communications and Networks (ICOCN). 2015, 1–3
83. Zheng J, Zhang M, Wang A, Wang Y. Photonic generation of ultrawideband pulse using semiconductor laser with optical feedback. Optics Letters, 2010, 35(11): 1734–1736
84. Zhang M, Liu T, Wang A, Zheng J, Meng L, Zhang Z, Wang Y. Photonic ultrawideband signal generator using an optically injected chaotic semiconductor laser. Optics Letters, 2011, 36(6): 1008–1010
85. Zhang M, Ji Y, Zhang Y,Wu Y, Xu H, Xu W. Remote radar based on chaos generation and radio over fiber. IEEE Photonics Journal, 2014, 6(5): 7902412-1–7902412-12
86. Ji Y, Zhang M, Wang Y, Wang P, Wang A, Wu Y, Xu H, Zhang Y. Microwave-photonic sensor for remote water-level monitoring based on chaotic laser. International Journal of Bifurcation and Chaos in Applied Sciences and Engineering, 2014, 24(03): 1450032-1–1450032-7
87. Han X, Wang L, Wang Y, Zou P, Gu Y, Teng J, Wang J, Jian X, Morthier G, Zhao M. UV-soft imprinted tunable polymer waveguide ring resonator for microwave photonic filtering. Journal of Lightwave Technology, 2014, 32(20): 3924–3932
88. Li W, Wang W T, Sun W H, Wang W Y, Zhu N H. Stable radio-frequency phase distribution over optical fiber by phase-drift auto-cancellation. Optics Letters, 2014, 39(15): 4294–4296
89. Li W, Sun W H, Wang W T, Wang L X, Liu J G, Zhu N H. Reduction of measurement error of optical vector network analyzer based on DPMZM. IEEE Photonics Technology Letters, 2014, 26 (9): 866–869
90. Li W, Zhu N H, Wang L X. Brillouin-assisted microwave frequency measurement with adjustable measurement range and resolution. Optics Letters, 2012, 37(2): 166–168
91. Venema L. Photonic technologies. Nature, 2003, 424(6950): 809
92. Azaña J, Madsen C K, Takiguchi K, Cincontti G. Special issue on “optical signal processing”. IEEE/OSA Journal Ligthwave Technology, 2006, 24(7): 2484–2767
93. Ngo N Q, Yu S F, Tjin S C, Kam C H. A new theoretical basis of higher-derivative optical differentiators. Optics Communications, 2004, 230(1-3): 115–129
94. Azaña J. Ultrafast analog all-optical signal processors based on fiber-grating devices. IEEE Photonics Journal, 2010, 2(3): 359–386
95. Slavík R, Park Y, Kulishov M, Morandotti R, Azaña J. Ultrafast all-optical differentiators. Optics Express, 2006, 14(22): 10699–10707
96. Park Y, Azaña J, Slavík R. Ultrafast all-optical first- and higher-order differentiators based on interferometers. Optics Letters, 2007, 32(6): 710–712
97. Ashrafi R, Li M, Azaña J. Coupling-strength-independent long-period grating designs for THz-bandwidth optical differentiators. IEEE Photonics Journal, 2013, 5(2): 7100311-1–7100311-12
98. Li M, Janner D, Yao J, Pruneri V. Arbitrary-order all-fiber temporal differentiator based on a fiber Bragg grating: design and experimental demonstration. Optics Express, 2009, 17(22): 19798–19807
99. Li M, Jeong H S, Azaña J, Ahn T J. 25-terahertz-bandwidth all-optical temporal differentiator. Optics Express, 2012, 20(27): 28273–28280
100. Li M, Yao J. Multichannel arbitrary-order photonic temporal differentiator for wavelength-division-multiplexed signal processing using a single fiber Bragg grating. Journal of Lightwave Technology, 2011, 29(17): 2506–2511
101. Li M, Shao L, Albert J, Yao J. Continuously tunable photonic fractional temporal differentiator based on a tilted fiber Bragg grating. IEEE Photonics Technology Letters, 2011, 23(4): 251–253
102. Ferrera M, Park Y, Razzari L, Little B E, Chu S T, Morandotti R, Moss D J, Azaña J. On-chip CMOS-compatible all-optical integrator. Nature Communications, 2010, 1(3): 29-1–29-5
103. Azaña J. Proposal of a uniform fiber Bragg grating as an ultrafast all-optical integrator. Optics Letters, 2008, 33(1): 4–6
104. Slavík R, Park Y, Ayotte N, Doucet S, Ahn T J, LaRochelle S,

Azaña J. Photonic temporal integrator for all-optical computing. Optics Express, 2008, 16(22): 18202–18214
105. Malacarne A, Ashrafi R, Li M, LaRochelle S, Yao J, Azaña J. Single-shot photonic time-intensity integration based on a time-spectrum convolution system. Optics Letters, 2012, 37(8): 1355–1357
106. Li M, Yao J. Ultrafast all-optical wavelet transform based on temporal pulse shaping incorporating a 2-D array of cascaded linearly chirped fiber Bragg gratings. IEEE Photonics Technology Letters, 2012, 24(15): 1319–1321
107. Li M, Yao J. All-optical short-time fourier transform based on a temporal pulse-shaping system incorporating an array of cascaded linearly chirped fiber Bragg gratings. IEEE Photonics Technology Letters, 2011, 23(20): 1439–1441
108. Li M, Yao J. Experimental demonstration of a wideband photonic temporal Hilbert transformer based on a single fiber Bragg grating. IEEE Photonics Technology Letters, 2010, 22(21): 1559–1561
109. Li M, Yao J. All-fiber temporal photonic fractional Hilbert transformer based on a directly designed fiber Bragg grating. Optics Letters, 2010, 35(2): 223–225
110. Ashrafi R, Li M, LaRochelle S, Azaña J. Superluminal space-to-time mapping in grating-assisted co-directional couplers. Optics Express, 2013, 21(5): 6249–6256
111. Ashrafi R, Li M, Belhadj N, Dastmalchi M, LaRochelle S, Azaña J. Experimental demonstration of superluminal space-to-time mapping in long period gratings. Optics Letters, 2013, 38(9): 1419–1421
112. Ashrafi R, Li M, Azaña J. Tsymbol/s optical coding based on long-period gratings. IEEE Photonics Technology Letters, 2013, 25(10): 910–913
113. Fernández-Ruiz M R, Li M, Dastmalchi M, Carballar A, LaRochelle S, Azaña J. Picosecond optical signal processing based on transmissive fiber Bragg gratings. Optics Letters, 2013, 38(8): 1247–1249
114. Li M, Dumais P, Ashrafi R, Bazargani H P, Quelene J, Callender C, Azaña J. Ultrashort flat-top pulse generation using on-chip CMOS-compatible Mach-Zehnder interferometers. IEEE Photonics Technology Letters, 2012, 24(16): 1387–1389
115. Li M, Li Z, Yao J. Photonic generation of precisely π phase-shifted binary phase-coded microwave signal. IEEE Photonics Technology Letters, 2012, 24(22): 2001–2004
116. Li Z, Li M, Chi H, Zhang X, Yao J. Photonic generation of phase-coded millimeter-wave signal with large frequency tunability using a polarization-maintaining fiber Bragg grating. IEEE Microwave and Wireless Components Letters, 2011, 21(12): 694–696
117. Li M, Yao J. Photonic generation of continuously tunable chirped microwave waveforms based on a temporal interferometer incorporating an optically pumped linearly chirped fiber Bragg grating. IEEE Transactions on Microwave Theory and Techniques, 2011, 59(12): 3531–3537
118. Li M, Han Y, Pan S,Yao J. Experimental demonstration of symmetrical waveform generation based on amplitude-only modulation in a fiber-based temporal pulse shaping system. IEEE Photonics Technology Letters, 2011, 23(11): 715–717
119. Li M, Shao L, Albert J, Yao J. Tilted fiber Bragg grating for chirped microwave waveform generation. IEEE Photonics Technology Letters, 2011, 23(5): 314–316
120. Li M, Wang C, Li W, Yao J. An unbalanced temporal pulse-shaping system for chirped microwave waveform generation. IEEE Transactions on Microwave Theory and Techniques, 2010, 58(11): 2968–2975
121. Wang C, Li M, Yao J. Continuously tunable photonic microwave frequency multiplication by use of an unbalanced temporal pulse shaping system. IEEE Photonics Technology Letters, 2010, 22 (17): 1285–1287
122. Weiner A M, Heritage J P, Kirschner E M. High-resolution femtosecond pulse shaping. Journal of the Optical Society of America B, 1988, 5(8): 1563–1572
123. Lepetit L, Chériaux G, Joffre M. Linear techniques of phase measurement by femtosecond spectral interferometry for applications in spectroscopy. Journal of the Optical Society of America B, 1995, 12(12): 2467–2474
124. Liu W, Li M, Guzzon R S, Norberg E J, Parker J S, Lu M, Coldren L A, Yao J. A fully reconfigurable photonic integrated signal processor. Nature Photonics, 2016: 190–195
125. Li M, Deng Y, Tang J, Sun S, Yao J, Azaña J, Zhu N. Reconfigurable optical signal processing based on a distributed feedback semiconductor optical amplifier. Scientific Reports, 2016, 6: 19985-1–19985-9

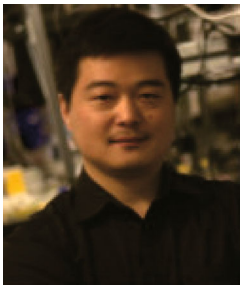

Ming Li (M'07) received the Ph.D. degree in electrical and electronics engineering from the University of Shizuoka, Hamamatsu, Japan, in 2009. In 2009, he joined the Microwave Photonics Research Laboratory, School of Electrical Engineering and Computer Science, University of Ottawa, Ottawa, ON, Canada, as a Postdoctoral Research Fellow. In 2011, he joined the Ultrafast Optical Processing Group under the supervision, INRS-EMT, Montreal, Canada, as a Postdoctoral Research Fellow. In 2013, he joined the Institute of Semiconductors, Chinese Academy of Sciences as a full-professor, under the support of "Thousand Youth Talents" program.

He has published more than 150 high-impact Journal and international conference papers. His current research interests include integrated microwave photonics and its applications, ultrafast optical signal processing and arbitrary waveform generation.

Ninghua Zhu (M'92) received the B.S., M.S., and Ph.D. degrees in electronic engineering from the University of Electronic Science and Technology of China, Chengdu, China, in 1982, 1986, and 1990, respectively. From 1990 to 1994, he was with Zhongshan University, Guangzhou, China, as a Postdoctoral Fellow, where he became an Associate Professor in 1992, and a Full Professor in 1994. From 1994 to 1995, he was a Research Fellow in the Department of Electronic Engineering, City University of Hong Kong. From 1996

to 1998, he was with Siemens Corporate Technology, Munich, Germany, as a Guest Scientist (Humboldt Research Fellow), where he was engaged in the microwave design and testing of external waveguide modulators and laser modules.

He is currently a Professor at the Institute of Semiconductors, Chinese Academy of Sciences (CAS), Beijing, China. During 1998, he was with the Hundred-Talent Program, CAS, and was selected by the National Natural Science Foundation as a Distinguished Young Scientist. He founded a Joint Photonics Research Laboratory between the Institute of Semiconductors, CAS, and City University of Hong Kong in 1998, and served as the Deputy Director. His research interests include modeling and characterization of integrated optical waveguides and coplanar transmission lines, and optimal design and testing of optoelectronics devices. He has authored or coauthored more than 170 journal papers, one book, and one book chapter.